Data-Driven Modelling & Forecasting of Chaotic Systems

B.L. Nortier

Abstract

It is a well-established practice to collect measurements from underlying artificial, natural, and physical systems through observables in order to realise a dynamical model with greater descriptive power. Many data-driven approaches to forecast the future evolution of systems exist. However, many of these methods rely on an initial understanding of the system and we often do not fully understand the many complexities of more intricate systems that we interact with on a daily basis.

In this project, the base assumption is that data is originates from some discrete-time dynamical system, particularly one of a chaotic nature but no assumptions are made pertaining to a specific dynamical system. A general learning problem is formulated and a well-known approach to the problem, alongside its practical limitations, is then considered. The notion of driven dynamical systems is introduced, and we subsequently establish the theoretical existence of a dynamical system possessing certain properties which guarantees it to be topologically conjugate ('dynamically equivalent') to the dynamics of the underlying system from which measurements were originally taken. Our methodology is implemented practically by making use of recurrent neural networks, a form of deep learning, to learn a map topologically equivalent to the underlying system that forecasts future states. In so doing we present the workability of an approach to obtain long-term topological and statistically consistent predictions for simple physical systems as well as a some chaotic attractors.

Contents

Chapter 1

Introduction

Experimenting with biological, physical, and artificial systems to generate a more informative dynamical model is a well-established practice in modern science. Traditional methods for modelling physical systems are based on laws of physics that are based either on empirical relationships or intuition. For systems that evolve with time, physical laws yield mathematical equations that govern how the quantities evolve with time. However, our world is much more complex than that which can be distilled into elegant equations. We do not fully understand many of the more complex systems, nor do they provide us with a good physical intuition of the underlying principles governing system dynamics. To complicate this, the underlying systems we observe often display sensitive dependence on initial conditions despite having highly similar initial conditions. This is because differing orbits diverge quickly and to such an extent that it becomes seemingly impossible to retrace their steps back to the original conditions. Even the presence of usually 'negligible' computational noise or measurement error renders long-term pointwise prediction infeasible. We encounter many difficultiesin the process of modelling such systems:

i. One may not have access to the complete states of the systems
ii. The system may be described by functions that behave wildly because their graphs have a wild oscillatory behaviour, i.e., a large functional complexity.

Models derived primarily from data can be classified into three categories:

i. Interpretable models (i.e., they establish relationships between internal physical mechanisms),
ii. Partially interpretable models capturing some modes of the dynamics,
iii. Non-interpretable models, defined as such mainly due to the fact that they are defined on a different phase space that is usually high-dimensional.

Examples in the literature attempting to forecast data from such systems have tried many different approaches with differing degrees of success. When we have complete access to states of the system,

an ordinary differential equation can be obtained from data ([**?**, **?**] and [**?**, **?**]) wherein one could approximate the vector field by a library of functions to obtain interpretable models.

Recent partially interpretable models available in the literature have been based on the Koopman operator (see [**?**, **?**]) to employ observables mapping the data onto a higher-dimensional space. This makes the dynamics in the higher-dimensional space more amenable for approximation by a linear transformation. Such methods do not guarantee exact reconstructions for nonlinear models, and in practice provide poor long-term consistency for a large class of chaotic dynamical systems [**?**].

The non-interpretable models include the delay embedding and the machine learning algorithms. For example, one could learn a system conjugate to the underlying system by applying the Takens delay embedding method of delay-coordinates [**?**] when one has "good" observations from the system; this learnt system could then be used to forecast the observed data. Takens delay embedding theorem [**?**] and its various generalisations (see, [**?**, **?**, **?**]) establishes the learnability of a system constructed by concatenating sufficiently large previous time-series observations of a dynamical system into a vector (called delay coordinates). This then confirms the existence of a map on the space of delay coordinates equivalent (or topologically conjugate) to the underlying map from which the observed time-series was first obtained. Although topological conjugacy guarantees an alternate representation of the underlying system, the quality still depends on numerous parameters, making the comprehension of the dynamics unreliable (see, [?]). One reason for this fragility is that the embedded attractor in the reconstruction space is not always an attractor of the map learnt in the reconstruction space, despite unquestionably being an invariant set. When the embedded object is not explicitly known to be an attractor (as explained in Chapter 3), it can cause predictions to fail.

Practically, the application of Takens embedding involves learning a map through some technique, and consequently one wishes that these would have low functional complexity[**?**], i.e., functions with fewer oscillatory graphs. On the other hand, pure machine learning methodology processes temporal information (like the echo state networks [**?**, **?**, **?**]) by mapping data onto a higher dimensional space for further processing. Although they perform well on forecasting some dynamical systems, they fail completely on others ([1]) as there is often no guarantee that the right function was learnt during training. EdN:1

This project involves implementing and analysing non-interpretable models that can guarantee exact reconstruction. The project work concerns the study and implementation of a method ([**?**]) that incorporates learning a function by mapping the data on to a higher dimensional space using what is called a driven dynamical system (See Chapter refch.4). With a clear understanding of how the data is mapped onto the higher dimensional space, the method then permits the learning of a dynamical system topologically conjugate to that of the underlying system. Instead of linear regression as in the training of echo state networks, deep learning methods are employed to learn the correct function. With slight modifications to the implementation in the paper ([**?**]), we show that one can construct accurate non-interpretable models with the ability to reconstruct attractors from

[1] EdNote: Ask for resources here

more hard-to-forecast systems like the double pendulum. (The forecasting of the time-series from a double pendulum has not been reported before.) Moreover, we also demonstrate that long-term statistical consistency is preserved.

By solidifying the mathematical underpinnings of our theory, we hope to guarantee the ability to construct models with predictive power ranging from molecular biology to neuroscience. in the near future. (We can modify this sentence when the report is completed.)

The more intricate details of proofs are referred to where relevant throughout. This report is organised as follows:
In Chapter 2, we recall the definition of a discrete-time dynamical system, how a discrete-system arises from a flow of an ODE and then proceed to define the inverse-limit space and topological conjugacy of autonomous systems.
Chapter 3 introduces the problem of forecasting dynamical systems, states the Takens delay embedding theorem, and discusses various issues faced while forecasting.
In Chapter 4, a driven dynamical system is defined and discuss the properties of a specific class of driven dynamical systems that we make use of in this project.
Finally, in Chapter 5 we show the implementation of these forecasting methods, and conclusions are provided in Chapter 6.

Chapter 2

Discrete-time Dynamical Systems

This chapter briefly describes a discrete-time dynamical system and what it means to exhibit chaos. We refer to [**?**, **?**] for more details.

At its most elementary level, a dynamical system is just something that evolves deterministically through time. In the context of this project, deterministic refers to the fact that a system evolves according to specified rules rather than based on random events. Dynamical systems arise in a variety of situations. A continuous-time dynamical system describes the states for all values of the time. Specifically, if the motion of a pendulum in which the quantities such as the angular position and angular momentum are known at all times, then it is a continuous-time dynamical system. The equations of the dynamical system can take the form of one or more ordinary differential equations that determine the relevant quantities at any future time if we know the initial location and momentum. In ecology, discrete-time dynamical systems are widely used to model population growth. The model in this case is a function calculating the following generation's population given the population of the previous generation. If we know the starting population, we may once again calculate the population at any time in the future.

Formally, a function $T : U \to U$, where U is some set is a *discrete-time dynamical system* and its iterates $\{u, Tu, T^2u, \ldots\}$, where T^n denotes the n-fold composition of T with itself, describe the evolution of an initial condition $u \in U$ (Note that we frequently drop the brackets and denote $T(u)$ by Tu so as to simplify notations).

Continuous-time dynamical systems modelled using ordinary differential equations can give rise to discrete-time dynamical systems. To see this, consider a differential equation $\dot{x} = f(x)$, $f : \mathbb{R}^n \to \mathbb{R}^n$, $n \in \mathbb{N}$ given to have a unique solution passing through each point $x \in \mathbb{R}^n$, call it $x(t)$ where $x(0) = x_0$.

Definition 1 (Flow of an Equation). The flow of the equation $\dot{x} = f(x)$ is defined to be a mapping $\varphi : \mathbb{R}^n \times \mathbb{R} \to \mathbb{R}$ where $\varphi(x_0, t) = x(t)$ for the solution $x(t)$ with $x(0) = x_0$

By fixing $t = K \in (0, \infty)$, we can define the *time-K map* as $T(x) := \varphi(x_0, K)$, and it is easily verified that $T \circ T(x_0) = \varphi(x_0, 2K)$. In general the m^{th} iterate of x_0 under T would be the value of the solution of the ODE evaluated at time mK with the initial condition x_0, i.e. $\varphi(x_0, mK)$. Thus ordinary differential equations give rise to a discrete-time dynamical system by sampling the value of the solution $x(t)$ at time intervals K units apart.

A numerical discretization of a differential equation can also give rise to a discrete-time dynamical system. For instance, Euler's method approximates $\dot{x}(t)$ by $(x(t+h) - x(t))/h$; if h is fixed throughout, the solution of a differential equation $\dot{x} = f(x)$ can be approximated at the time instant $t + (m+1)h$ by iterating the equation

$$x(t + (m+1)h) = x(t + mh) + hf(x(t + mh)) \tag{2.1}$$

Adopting more succinct notation by replacing $x(t + mh)$ with u_m, we rewrite the above equation as

$$u_{m+1} = u_m + hf(u_m) \tag{2.2}$$

or in even simpler terms as the discrete-time dynamical system with map $T(u) = u + hf(u)$, where T, u and f are understood to be as above.

Of course, discrete-time dynamical systems need not always arise through a differential equation. Once again, we may consider the field of ecology, where discrete dynamical systems are often directly
EdN:2 derived or assumed. [2] There is a school of thought that advocates discrete-time dynamical systems to be more natural for modelling real-world observations than differential equations. We refer the interested reader to [**?**].

2.1 Invariant Sets

A core concept in the study of dynamical systems is that of invariance.

Definition 2 (Invariant Set). Given a discrete-time dynamical system $T : U \to U$, a subset $A \subset U$ is said to be an *invariant set* if $T(A) = A$.

We also define the orbit of a function T.

Definition 3 (Orbit of T). The orbit of T is to be defined the sequence $\bar{u} = \{u_n\}_{n \in \mathbb{Z}}$ obeying the update equation, $u_{n+1} = Tu_n$, $n \in \mathbb{Z}$.

[2] EdNote: Ask for resource

Two examples of invariant sets include a fixed point where $Tu = u$ for $u \in U$, and a periodic orbit, i.e., a set of iterates $\{u, Tu, T^2u, \ldots, T^pu\}$, where $T^{p+1}u = u$ for some $p \in \mathbb{Z}$. The entire space U could be also be invariant. Consider for example the space $U = [0, 1]$, where $Tu = 4u(1-u)$ and then U is invariant (as every $u \in U$ can be written as $u = 4x(1-x)$ for some $x \in U$).

We may learn a great deal about the iterates of a dynamical system by considering the types of invariant sets of a discrete-time dynamical system. For example, if $U = [0, 1]$ has map $Tu = u/2$, then the only invariant set is $\{0\}$, and all orbits approach this invariant set as time flows in the forward direction. Indeed, if a some non-zero invariant set (call it B) exists, then there is some $r \in (0, 1] \cap B$. But $r \notin T(B)$ since any orbit with initial value r will be a decreasing sequence. Moreover, every orbit of T will be decreasing and therefore approach the value 0 as $n \to \infty$.

One may ask if every orbit approaches an invariant set? In general the answer is no, since for the dynamical system $T : \mathbb{R} \to \mathbb{R}$ defined by $Tu = 2u$, any orbit that does not intersect the invariant set $\{0\}$, will not approach any invariant set.

However, when the space U is compact, all orbits approach an invariant set. This is since the set of limit points of the orbit can be shown to be invariant [**?**]. So, when U is compact, the ω-limit set $\omega(u; T)$ of a point u defined to the collection of limit points of the sequence $\{x, Tu, T^2u, \ldots\}$ is nonempty, and $\omega(u; T)$ is invariant.

Example 1. *For the map $Tu = u^2$ defined on $[0, 1]$ all orbits lie in the invariant set $\{1\}$ or else would would approach the invariant set $\{0\}$.*

Invariant sets have various properties. Invariant sets can be attracting or repelling depending on how orbits in their vicinity behave. Recall the examples $Tu = u/2$ and $Tu = 2u$ defined on $\mathbb{R}$ (where $\{0\}$ "attracts" orbits) or the example, $Tu = u^2$ defined on $[0, 1]$ (where $\{1\}$ "repels" orbits). We are interested in attractive invariant sets since they capture the long-term dynamics as time increases. In particular, we are interested in those invariant sets named attractors.

Definition 4 (Attractor). Let $T : U \to U$, where U is a metric space with metric d. A compact subset $A \subset U$ is said to be an attractor if it satisfies the three conditions:

1. A is invariant.
2. A is asymptotically stable, i.e., for every $\epsilon > 0$ and for all u so that $d(u, A) < \epsilon$, we have $d(T^nu, A) \to 0$ as $n \to \infty$.
3. A has Lyapunov stability, i.e., for every $\epsilon > 0$ there exists a $\delta(\epsilon) > 0$ so that $d(u, A) < \delta$ implies $d(T^nu, A) < \epsilon$ for all $n \geq 0$.

Indeed in our previous examples, it can be verified that the system $Tu = u/2$ defined on $\mathbb{R}$ and $Tu = u^2$ defined on $[0, 1]$ the singleton set $\{0\}$ is an attractor. For the system, $Tu = 1 - |2u - 1|$ on $[0, 1]$, one may easily verify that the only attractor is the entire space $[0, 1]$. This follows from

the fact that between any two points $u < v$ in $[0, 1]$, and for any a, b so that $u \leq a < b \leq v$, we can find an n so that $T^n(a, b) = [0, 1]$ (as would be explained later in this chapter).

A dynamical system can have several attractors and may also be contained in another attractor. For the example, $Tu = u^2$ on $[0, 1]$, both $\{0\}$ and $[0, 1]$ are attractors. It is known that an attractor for a dynamical system always exists in a compact space [**?**].

The dynamics restricted to an invariant set can be complicated. For instance an invariant set could be just a single point or it could have an infinite set. If the invariant set is infinite, then complicated dynamics are possible. A particular, well-studied phenomenon of such complexity gives rise to so-called chaotic behaviour, a subject studied in detail over the past fifty years.

2.2 Chaos

In the 1960s, several mathematicians and mathematically interested scientists independently discovered chaos in the mathematical sense. The meteorologist Edward Lorenz may have been the first to explain this phenomenon in his 1963 paper [**?**]. The notions of invariance, attractivity, and chaos may also be described for continuous systems, and Lorenz's system comprised of a system of differential equations. The narrative of Lorenz's discovery of chaos and the history of other forerunners in this subject is fascinating. We highly recommend James Gleick's book Chaos: The Making of a New Science [**?**] for those interested. It clearly illustrates these experiences, explains why chaos was such a startling and crucial mathematical and scientific discovery and describes the underlying mathematical notions for non-specialists.

Different authors propose a number of intricately different definitions of chaos in the literature [**?**, **?**, **?**] and each of them indicate some aspect of complexity.

In practice, when only data is observed from a system, it is not possible to verify which definition or notion is satisfied by the underlying dynamical system. We do, however, specifically recall the definition of chaos in the sense of Devaney [**?**, **?**] so as to understand some nuances behind the complexity. Devaney's definition of chaos has three requirements, with the first being the notion of sensitive dependence on initial conditions.

Definition 5. [**Sensitive Dependence on Initial Conditions**]A dynamical system $T : U \to U$ is said to have sensitive dependence on initial conditions (SDIC) if there exists a $\delta > 0$ such that for every $u \in U$ and in every neighborhood of $u \in U$ there exists a $v \in U$ and an integer $N := N(u, v) \in \mathbb{Z}$ such that $d(T^N u, T^N v) > \delta$.

It is vital to acquire a sense of this definition as it can easily be misunderstood. It is a common misconception to interpret SDIC as two close points (u and v) that eventually become separated

by a distance δ under iteration by T. But this is not true. To fully comprehend all the subtleties of the concept, one needs to discuss it more thoroughly by considering each sentence with care and attention, whereafter one may examine how they fit together to convey the idea of sensitive dependence.

To this end, we make 3 remarks:

1. First, the $\delta > 0$ in the definition of SDIC is independent of u.
2. Second, in every neighborhood of u, we may not necessarily find all points v in the neighborhood distinct from u that would separate from the forward iterates of u.
3. Finally, N depends upon u and v chosen, and their iterates may not separate forever (i.e., for all $n > N$) and we allow their iterates to get arbitrarily close in the future.

To illustrate the concept of SDIC, we present two examples - one from Mathematics and the other from the field of Physics.

Example 2. The logistic map(LM), a recursion relation of the form $x_{n+1} = rx_n(1 - x_n)$ where $x_n \in [0, 1]$ and $r \leq 4$ is a classic example used to illustrate the chaotic behaviour that a system may exhibit. When $r = 4$, the one-dimensional recurrence relation $x_{n+1} = 4x_n(1 - x_n)$ can be used as the kindergarten's model to exhibit the presence of SDIC. [3] In the graph below 1 we plot the first 50 iterates of the LM for $r = 4$ and two slightly different initial values x_0. EdN:3

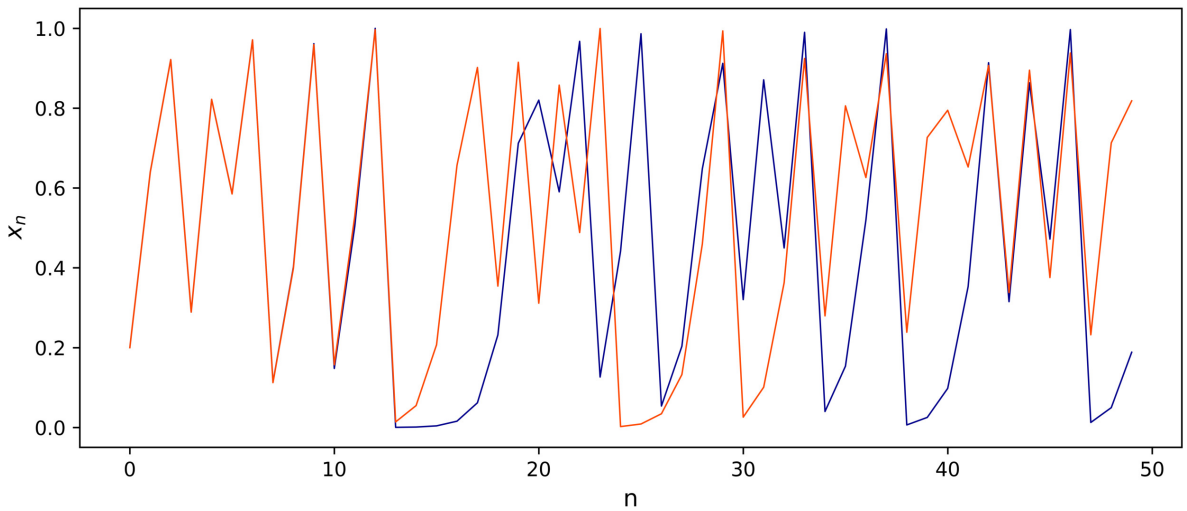

Fig. 1. Figure generated for Logistic Map $x_{n+1} = rx_n(1 - x_n)$ with $r = 4$ to exhibit the presence of SDIC. Plotted are the values x_n against time n for the the first 50 step with initial values $x_0 = 0.2$ (blue) and $x_0 = 0.20001$ (red). Initially the two trajectories overlap, but they diverge completely at $n = 12$ whereafter they follow distinct paths.

4 EdN:4

[3] EdNote: B: edited and removed unnecessary citation
[4] EdNote: B: Caption and figure adjusted

Example 3. A second example pertains to a simple physical system called the double pendulum - a pendulum with another pendulum attached to its head given an initial position and angular velocity.

Below are two figures denoting trajectories of a double pendulum's second head after some elapsed time. Depicted are three pendulum heads with equal angular velocity but differing slightly in initial position. As can be seen below, the trajectories diverge very quickly to become completely different. We discuss the double pendulum in greater detail in a later chapter (5), but we mention the example here to provide a numerical example of a practical system exhibiting SDIC.

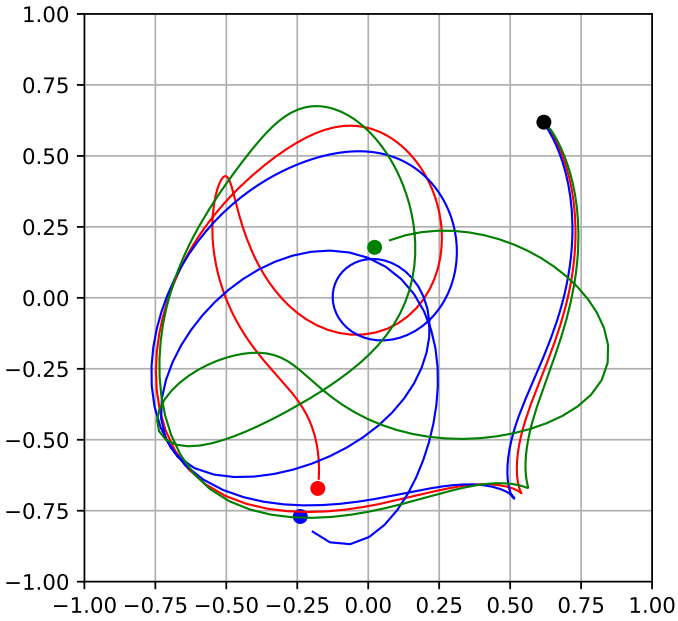

Fig. 2. Three double pendulum heads with equal angular velocity and initial angles differing by 0,025 radians

The second part in Devaney's definition of chaos concerns topological transitivity.

Definition 6 (Topologically Transitive). A dynamical system $F : U \to U$ is topologically transitive if for any pair of nonempty open sets E_1 and E_2 there exists a $n \in \mathbb{N}$ such that $T^n(E_1) \cap E_2 \neq \emptyset$.

Topological transitivity implies that iterates of an open set of initial conditions get mixed up with other open sets. On a compact metric space, one may show that topological transitivity also implies the existence of a point whose forward iterates are dense [**?**]; or in other words, the orbit going through this point will be dense in the compact metric space. In fact, it is topologically more likely that the choice of an arbitrary point will be one whose iterates are almost dense.

Definition 7 (**Meager Set).** A subset of a topological space U is said to be a meager set if it can be written as a countable union of sets of with empty interior. The complement of the a meager set is set to be a residual set.

To be more precise (see [**?**]), for a discrete-time dynamical system on a compact space, the set of points with dense iterates are residual, and they are typical or likely to be observed in practice. In this project, when data is observed from a topologically transitive system, we assume it arises from a dense orbit.

We may now define the notion of Chaos as formulated by Devaney[**?**].

Definition 8 (**Devaney's Chaos).** A dynamical system $T : U \to U$ is said to exhibit chaos in the sense of Devaney if it satisfies the three properties:

1. T has SDIC.
2. T is topologically transitive.
3. The set of periodic points of T are dense in U.

Example 4. The standard tent map $Tu = 1 - |2u - 1|$ defined on $[0, 1]$ is a well-known example of a dynamical system satisfying these three properties.

We now reason as to why this is true. The graph of the map T is piecewise linear with two straight lines, one connecting the points $(0, 0)$ and $(\frac{1}{2}, 1)$ and the other connecting $(\frac{1}{2}, 1)$ with $(1, 0)$. They form a so-called tent with base centered at $u = 1/2$. The graph of the map T^2 comprises two symmetric tents with their base centered at $1/4$ and $3/4$. See Figure 3

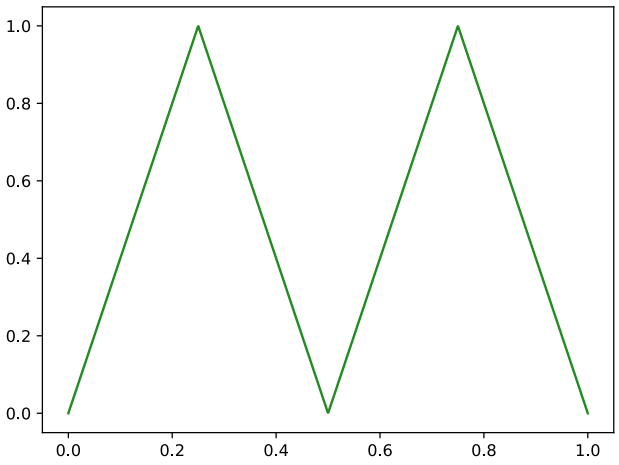

Fig. 3. Graph of the T^2 map with bases at $x = 0$, $x = \frac{1}{2}$ and $x = 1$ respectively.

In general, the graph of T^k contains 2^{k-1} tents. Given any point u and an open neighborhood $W \subset [0,1]$ of u, we can find $k \in \mathbb{Z}$ large enough so that $T^k(W) = [0,1]$ because we can accommodate a tent whose base is contained in W. This implies the existence of two points w_1 and w_2 in W so that $d(T^k w_1, T^k w_2) = 1$, and by the triangle inequality at least one of the inequalities $d(T^k u, T^k w_1) > \delta$ or $d(T^k u, T^k w_2) > \delta$ hold when $\delta \in (0, \frac{1}{2})$. So T has sensitive dependence on initial conditions.

Next, let W_1 and W_2 be two nonempty open sets. Given any open set W_1, we can find a $k \in \mathbb{N}$ large enough so that $T^k(W_1) = [0,1]$ because we can accommodate a tent with base contained in W. So $T^k(W_1) \cap W_2 \neq \emptyset$, and thus T has topological transitivity.

Finally, for every open interval (a,b), the graph of T^k intersects the graph of the identity map on $[0,1]$. This follows from the fact established above that there exists a $k \in \mathbb{N}$ such that $T^k(a,b) = [0,1]$.If the intersection point has coordinates of the form (p,p), the point p is then a fixed point of T^k and therefore also a periodic point of T. Since we have found a periodic point in the interval W, the set of periodic points are dense in T. This follows because any fixed point of T^k is also a periodic point, and we have found this in an arbitrary interval.

2.3 Conjugacy

We now turn our attention to the subject of conjugacy that describes when two dynamical systems are equivalent dynamically.

To show topological similarity (or sameness) between two metric or topological spaces, one needs to establish a homeomorphism between the two spaces. However, in the study of dynamical systems defined on two spaces, establishing a homeomorphism does not indicate that the systems are dynamically related in any way. For instance, the maps $Tu = u^2$ and $Tu = 1 - |2u - 1|$ defined on $[0,1]$ have totally different behaviour. Therefore, to find dynamically similar systems, one must establish a dynamical equivalence that we illustrate in a simple commutativity diagram below 2.3.

$$\begin{array}{cc} U & U \\ & \\ V & V. \end{array} \tag{2.3}$$

To understand the diagram, we note that if we travel "right and then down," the diagram instructs us to use T (top arrow right) first, followed by ϕ. (right arrow downwards). Consequently, the pathway amounts to finding $\phi(T(u))$. If we proceed "down and then right," the diagram instructs us to apply ϕ (left arrow downwards) first, and then apply S (bottom arrow right). This then amounts to finding $S(\phi(u))$. When the relationships in this diagram hold, we say $\phi(T(u)) = S(\phi(u))$, and we formally denote it as $\phi \circ T = S \circ \phi$.

Definition 9. [**Conjugacy & Semi-Conjugacy**]Consider the dynamical systems $T : U \to U$, $S : V \to V$ and suppose the relationship $\phi \circ T = S \circ \phi$ holds. If $\phi : U \to V$ is a homeomorphism, then S is said to be conjugate to T and ϕ is called a conjugacy. If we relax the criterion on ϕ and merely require ϕ to be continuous and surjective where $\phi : U \to V$, then ϕ is a semi-conjugacy between T and S where T has domain U and S has domain V; S is said to be semi-conjugate to T.

[5] When S is conjugate to T, the dynamics of the two systems are in some way 'dynamically equivalent'. Specifically, they are in one-to-one correspondence with one another. However when S is semi-conjugate to T with $\phi : U \to V$ a many-to-one mapping, the dynamics on V provide merely a coarse-grained description of the dynamics on U [**?**]. When S is semi-conjugate to T, it is also common to call S a *factor of* T, or conversely that T is an *extension of* S. In essence, an extension (see, [**?**]) is a more extensive system capturing all of the essential dynamics of its factor. EdN:5

It is a very hard or nearly an impossible task to establish the existence of a conjugacy or a semi-conjugacy ϕ between two systems [**?**]. However, one can verify that a function ϕ satisfies the commutativity diagram 2.3.

Example 5. For example $\phi(x) = \sin\left(\frac{\pi}{2}x\right)^2$ is a conjugacy between two systems $Tu = 1 - |2u - 1|$ and $Sv = 4v(1 - v)$ defined on $U = [0, 1]$.

Indeed, $\phi : [0, 1] \to [0, 1]$ is a homeomorphism and by employing simple trigonometric identities, it is easily proved that ϕ satisfies 2.3

$$\begin{aligned}(\phi \circ T)u &= \sin^2\left(\frac{\pi}{2} - \frac{\pi}{2}|2u - 1|\right) = \sin^2(\pi u) = \left(2\sin(\frac{\pi}{2})\cos(\frac{\pi}{2})\right)^2 = 4\sin^2(\frac{\pi}{2}u)\left(1 - \sin^2\frac{\pi}{2}u\right) \\ &= (S \circ \phi)u.\end{aligned}$$

And it follows that ϕ is a conjugacy between the two systems.

By establishing that two systems are conjugate (semi-conjugate) to one another, we have also shown that one may choose to work with one system instead of the second and still be guaranteed to obtain information on the latter. It is instrumental during the process of forecasting the future evolution of dynamical systems.

[5] EdNote: B: Does defining explicitly the domain and codomain of ϕ make it clear enough? M: Saying ϕ is then a semi-conjugacy between T and S could be ambiguous as it does not specify which system is on the top in the commutativity. So please edit accordingly.

Chapter 3

The Learning Problem

In this chapter, we acquaint ourselves with the question of forecasting dynamical systems with unknown underlying structures, state and discuss the shortcomings of the Takens delay embedding theorem and discuss various issues faced while forecasting.

Consider a relatively simple learning problem: Given the sequence $(u_0, u_1, \ldots, u_m)$ for $m \in \mathbb{Z}$, a finite segment of an orbit of the map T where T is defined by the update equation $u_{n+1} = Tu_n$, forecast the values u_{m+1}, u_{m+1} where the map T is unknown, given that u_m.

A practical example of this would be the subsequent scenario: given the time-sequential coordinates of an object moving in space, predict the future positions of that object. We are very rarely, if at all, presented with a problem where the entire state information is available to us in the form u_n at some timestep $n \in \mathbb{N}$. Consider then a more complicated learning problem:

Suppose we only have the observations $\theta(u_0), \theta(u_1), \ldots, \theta(u_m)$ of the true system states u in an unknown dynamical system (U, T) and we wish to predict the values $\theta(u_{m+1}), \theta(u_{m+2})$ and so forth.

EdN:6 First we establish the method of Takens delay embedding. In this method, one considers a discrete-time dynamical system defined on a 'nice' space (a smooth manifold)[6] that can be obtained as time-K map of a continuous time-dynamical system, concepts formalised below. We make observations from such a system, i.e., we observe the evolution of $\theta(w_0)$ (where w_0 represents the initial state) by examining a finite set of values of $u_n := \theta(w_n) = \theta(Tw_{n-1})$. The sequence $\{u_n\}$ represents a scalar time-series and intuitively θ represents a probe inserted into a bigger system which is itself only measuring/extracting a small part of the greater system state at time $t = n$. Consider, for example, a thermometer erected to measure the ambient temperature in a local village. This measurement function, the thermometer, is capturing only a single aspect, the temperature,

[6] EdNote: B: Should this be further explained?

of a much grander dynamical system entailing the current weather of the surrounding area. Even more than that though- it is measuring a miniscule part of the global weather system.

However, the actual state u of a system is seldom, if ever, fully known. the most one can do is to insert probes into a system to obtain partial information through the measurements taken. Moreover, the process of taking a measurement itself introduces two additional aspects which complicate the problem: [7] EdN:7

i. A series of measurements over a specific time interval is inherently a discretisation procedure of the underlying continuous-time dynamical system. (Hence why we restricted our attention to discrete-time systems in the preceding section)
ii. A probe will never be entirely accurate, and so the act of measurement introduces a certain measure of numerical noise/inaccuracy.

From here we construct a multidimensional observable using the method of stacking previous observations, i.e., we create delay-coordinate map defined by $\Phi_{k,\theta}(w) := (\theta(T^{-k}w) \ldots, \theta(T^{-1}w), \theta(w))$. The concept of an observable is understood in the sense of an observable as originally introduced by [**?**, **?**] to refer to a probe or measurement function inserted into the system. Takens' theorem, in essence, refers to the fact that for a sufficiently large k, we can define a dynamical system on the space $\mathbb{R}^{k+1}$ with states $\Phi_{k,\theta}(w)$, $\Phi_{k,\theta}(Tw)$, $\Phi_{k,\theta}(T^2w)$, etc. This dynamical system is topologically conjugate to the unknown underlying system (W, T). We recall the Takens delay embedding theorem next.

3.1 Takens Embedding Theorem

We define first the concepts of homeomorphism and embedding:

Definition 10. [**Homeomorphism**]A homeomorphism is a function $f : Z \to Y$ between two topological spaces Z and Y that is continuous, bijective and has a continuous inverse.

Definition 11 (**Embedding).** Consider a homeomorphism $f : Z \to Y$ for $Y \subset X$. Z is said to be embedded in X by f.

Takens Theorem states a result establishing a relationship between the observed and underlying dynamical systems by showing that the concatenation of a sufficiently large number of previous observations into a vector will, under certain conditions, generate a map between the vectors from the respective systems. We formulate the theorem from [**?**].

[7] EdNote: B: Perhaps this edit makes more sense? M: Maybe replace difficulty by saying that we need to consider two aspects.

Theorem 1 (**Takens Embedding Theorem (adopted from [?]).** *Let W be a compact manifold of dimension m, and $d \geq m$ so that $2d$ is an integer. It is a generic property for the pair (T, θ), where $T : W \to W$ is a smooth diffeomorphism, and $\theta : W \to \mathbb{R}$ a smooth function, the map $\Phi_{2d,\theta} : W \to \mathbb{R}^{2d+1}$ defined on W by $\Phi_{2d,\theta}(w) := (\theta(T^{-2d}w) \ldots, \theta(T^{-1}w), \theta(w))$ is a diffeomorphic embedding; by 'smooth' we mean at least C^2. Consequently, there exists a map $F_\theta : \Phi_{2d,\theta}(W) \to \Phi_{2d,\theta}(W)$ defined by*

$$F_\theta : (\theta(T^{-2d}w), \ldots, \theta(T^{-1}w), \theta(w)) \mapsto (\theta(T^{-2d+1}w), \ldots, \theta(w), \theta(Tw))$$

so that (W, T) is topologically conjugate to $(\Phi_{2d,\theta}(W), F_\theta)$.

By generic we mean a residual set on a certain topology on appropriate spaces of functions (that
EdN:8 we do not describe here) [8]. By C^2, we make reference to a twice-differentiable function with a continuous second derivative. In our scenario (and this remains important throughout) the input space U is considered the attractor.

Below we reproduce Figure 1 from [**?**].

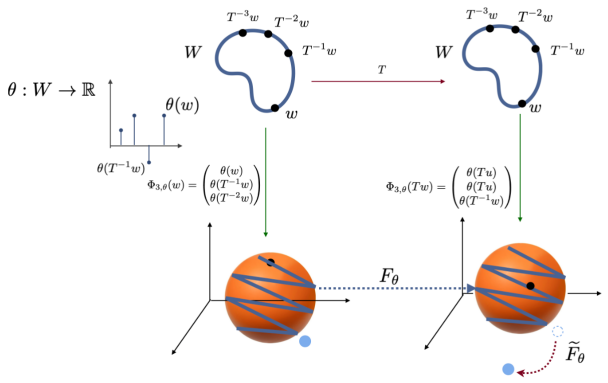

Fig. 1. Schematic of Takens Embedding Theorem's usage and impact of iterates slipping from the attractor when the approximation $\tilde{F}_\theta$ of F_θ is learnt.

If we can learn the map F_θ, from sufficient number of data points of $\{\phi_{2d,\theta}(w_n)\}$, then we also know how to forecast how $\theta(w_n)$.

3.2 Practical Limitations to Takens' Theorem

Takens' Embedding Theorem is a powerful result, and it provides compelling reason to believe that one could conceivably reconstruct a system conjugate accurately to the underlying system. ~~Nonetheless, it does present some severe~~ practical limitations:

[8] EdNote: B: Where can I find a citation for this?

1. Even supposing that we could indeed find F_θ , our *approximation* of F_θ is a map from a larger set $\mathbb{R}^{2d+1}$ containing the embedded attractor. There are, however, no theoretical guarantees that F_θ will retain $V = \Phi_{2d,\theta}(W)$ as an attractor although W could itself be an attractor.

2. Takens theorem is stated only for noiseless observations. Due to noise ϵ_n the delay vector $\Phi_{2d,\theta}(w_n) + \epsilon_n$ may lie outside V.Furthermore, due to the chaotic nature of the underlying system (i.e. the fact that it has SIDC), the evolution of $\Phi_{2d,\theta}(w_n) + \epsilon_n$ under the map F_θ could move out of V completely. This problem can be overcome by using a driven dynamical system with some properties, and we discuss this in Chapter3.

Though not a uniquely related to the Takens embedding theorem, we do opt to make mention of another requirement for our work. The methods described here are applicable for data originating from a surjective map. This follows from the fact that when T maps the space U into a proper subset B ofU, there exists some point in $U - A$ that does not have a preimage and we conclude that T is not surjective. An example of this would be the case when a system displays energy-loss. Consider, for instance, consider the dying oscillations for a damped pendulum. (An account of greater depth is provided in 5)

This requirement is not overly restrictive, as a great number of chaotic systems do have a surjective map. (Cite) [9] EdN:9

[9] EdNote: B: I remember you saying this in one of our sessions, but don't have a source for it. Do you have a specific reference?

Chapter 4

Driven Dynamical Systems to Forecast Problems

In this chapter, we discuss results on the mapping of temporal data obtained from a discrete-dynamical system onto a different space through the notion of a driven dynamical system. We also consider the conditions a driven system should possess to avoid adding distortion to its state-space representation. We then describe the *single-delay dynamics* (SDD) of the system and finally recall conditions on the driven system so that the SDD are conjugate (or at least semi-conjugate) to the underlying system. The SDD can then be used to forecast and reconstruct the underlying system.

4.1 Nonautonomous and Driven Dynamical Systems

Definition 12 (**Nonautonomous Dynamical System (adopted from** [?]**)).** A nonautonomous dynamical system (NDS) on a space X is simply a dynamical system comprising a family of maps $\{g_n\}_{n\in\mathbb{Z}}$ where $g_n(.) := g(u_n, .) : X \to X$ is continuous. Each g_n arises as a consequence of an input u_n from the input space U, a topological space.

We immediately recall the figure first defined in (2.3) and remind ourselves of our ultimate goal to learn a system that is conjugate to an underlying or unknown dynamical system (U, T) by making use of the measurements obtained from the unknown system.

U U

V V.

To find a function ϕ, the need now arises to consider a so-called driven dynamical system, a special case of a nonautonomous dynamical system. Two spaces are considered: input is taken from an input space U and the state of a space X is updated. (Previously, only the state was considered.) We do this to mimic the true conditions. By accounting for an extrogenous input sequence in U which can also influence the system-state at a specific time-step, it produces more general models than an autonomous system.

Definition 13 (**Driven, Compactly Driven Dynamical System).** A driven dynamical system comprises two topological metric spaces U, X and a continuous function $g : U \times X \to X$ where $g(u_n, x_n) = x_{n+1}$. If the input space U is compact, we refer to the system as compactly driven.

The update equation $x_{n+1} = g(u_n, x_n)$ for $n \in \mathbb{Z}$, input u_n from U and state x_n belonging to X (a compact space) generate the dynamics on X. Abbreviated, we refer only to the *driven system* g, where all other entities are understood implicitly.

Notably, a nonautonomous dynamical system can be generated from U; any input $\overline{u}$, a bi-infinite sequence from U, gives rise to the sequence of self-maps $\{g(u_n, \cdot)\}_{n\in\mathbb{Z}}$ contained in X. Physically, one may think of this bi-infinite sequence as referring to a system that has been running for an extended period at the time of the first measurement taken from the system (alternatively, the first time a probe is inserted into the system to take an observation)

Definition 14 (**Entire Solution).** A sequence $\{x_n\}_{n\in\mathbb{Z}} \subset X$ is called an entire solution (or simply a solution) of the driven system g with input $\overline{u}$ when it satisfies

$$g(u_{n-1}, x_{n-1}) = x_n$$

for all $n \in \mathbb{Z}$

It is important to emphasise that a sequence $\{x_n\}$ satisfying the update equation above can only be a solution if $x_n \in U$ holds for all $n \in \mathbb{Z}$ and just for $n > 0$. Consider the example below.

Example 6. The only solution $\{x_n\}_{n\in\mathbb{Z}}$ to the driven system $g(u, x) = \frac{ux}{2}$, where $X = [0, 1]$, $U = [0, 1]$, is the zero solution $x_n \equiv 0$. To see this, consider any $x_n = a \in [0, 1]$ where $a \neq 0$. Let $\overline{u} \in U$ be an non-zero constant sequence , say $u_n = 0.5$. The driven system may be rewritten as $x_{n-1} = \frac{2x_n}{u_{n-1}} = 4x_n$ and the iterates of x_n in backward time will increase by a factor of 4 at each timestep. Thus for some $m \leq n$, $1 < x_m$ i.e. $x_m \notin X$. So $\{x_n\}_{n\in\mathbb{Z}}$ is not a solution and it follows that the only possible solution is the zero solution.

A system may also have multiple solutions, as evidenced in the example below.

Example 7. Consider the driven system $g(u, x) = x^2$ for $X = [0, 1]$, $U = \mathbb{R}$. The system has an uncountable number of solutions, as there exists a solution for every $x \in X$ which also passes through the point x and $lim_{n\to\infty} x_n = 0$, $lim_{n\to-\infty} x_n = 1$. The proof is deferred to immediately after the next paragraph (see 1).

As the solutions to a driven system are considered an important entity, we next identify a subspace X_U of X that contains all possible solutions. To realize such a subspace of a driven system g, the concept of a reachable set is defined.

Definition 15 (Reachable Set). The reachable set of a driven system g is exactly the union of all the elements of all the (entire) solutions, i.e.,

$$X_U := \Big\{ x \in X : x = x_k \text{ where } \{x_n\} \text{ is a solution for some } \bar{u} \Big\}.$$

The set of all reachable states at a specific time n for input $\overline{u}$ is denoted by $X_n(\overline{u})$

The reachable set itself can defined independently from g possessing the ESP/USP. Note that $x \in X_n(\overline{u})$ if and only g has a solution $\{x_k\}$ for $x_n = x$ and input $\overline{u}$, a result proved in nonautonomous dynamical systems literature [**?**, **?**]. [10]

EdN:10

The set $X_n(\overline{u})$ is precisely the set of points x through which some entire solution Ψ passes at time n. We can give an alternate formulation of the set $X_n(\overline{u})$. Now suppose, we for some fixed input $\overline{u}$, we define $g_i = g(u_i, \cdot)$ for all $i \in \mathbb{Z}$, then the set of states

$$X_{n,i}(\overline{u}) := g_{n-1} \circ \cdots g_{i+1} \circ g_i(X). \tag{4.1}$$

The set $X_{n,i}(\overline{u})$ being the image of a finite composition of continuous maps is compact whenever X is compact. Also $X_{n,i}(\overline{u})$ is nonempty. Further, $X_{n,i}(\overline{u}) \supset X_{n,i-1}$. Hence $\bigcap_{i<n} X_{n,i}(\overline{u})$ is a nested intersection of closed nonempty subsets, and whenever X is compact, the intersection is nonempty. We say g is a topological contraction if $\bigcap_{i<n} X_{n,i}(\overline{u})$ is a singleton subset of X for each $\overline{u}$.

It turns out that $\bigcap_{i<n} X_{n,i}(\overline{u})$ is identically equal to $X_n((\overline{u})$ that we had defined earlier. This will lead to a result (for. see, [**?**]) that *g being a topological contraction is equivalent to the existence of a exactly one entire solution.*

Remark 1 (Proof of Example 7). For the driven system, $g(u, x) = x^2$ the evolution does not depend on the input at all. Hence $g(u, x)$ can be written as a single map $f(x) = x^2$ which is a homeomorphism on $[0, 1]$. A left-infinite orbit is defined and it converges to 1 while the right-infinite orbit converges to 0. Or in other words the iterates of f^{-1} converges to 1 while the iterates of f converge to 0

Thus far, it has been demonstrated that a system may have one or more solutions; one may ask if a driven system always has a solution and, if so, whether it satisfies specific properties such as uniqueness. Should the driven system be compact, existence follows immediately, as shown in the following result.

[10] EdNote: B: Adjusted sentence and cited

Theorem 2. *Let g be a driven system. If X is compact then for each input $\overline{u}$, there exists at least one solution to the driven system $g(.\,, x)$*

Proof. May be found in [**?**, **?**, **?**] □

4.2 Unique Solution Property

Definition 16 (**Unique Solution Property).** A driven system g is said to have the Unique Solution Property (USP) if for each input $\overline{u}$ there exists exactly one solution. Alternatively we may formulate the USP as follows: g has the Unique Solution Property if there exists a well-defined map $\Psi : U \to X$, with $\Psi(\overline{u})$ denoting the unique solution.

One of the first results obtained after defining the USP is that every solution will attract different initial conditions towards the component parts of the solution. If g has the USP, then any solution to g is also a uniform attractor in nonautonomous dynamical systems literature [**?**]. The discussion on nonautonomous attractors is beyond the scope of this project, and we refer the reader to [**?**, **?**] for further reading.

In the majority of Reservoir Computing(RC) literature (a machine learning approach) where the input is mapped onto a different but higher dimensional through a system called the reservoir and a readout that measures the state of the reservoir is trained, a notion of forgetting the states of the reservoir asymptotically is often used.

Concepts like the ESP, fading memory [**?**] are some of these notions. If g possesses the ESP (equivalent in our context to the USP), the we are guaranteed that the whole of an input's left-infinite history will exactly determine the current system state; i.e. there is only ever the possibility of a single reachable state at a given instance of time [**?**, **?**].

Beyond forgetting the past states the ESP is also often discussed in terms of a stability property that is nearby inputs create close by responses (solutions), a concept called input-related stability [**?**] and, furthermore, plays a key role in the robustness of recurrent neural networks(RNN), a component of the implementation discussed in 5.

4.3 Conjugacies

Having already defined the reachable set X_U as the collection of all elements of all entire solutions, we pause briefly in order to fix additional notation. Defining $\overleftarrow{u}^n := (\ldots, u_{n-2}, u_{n-1})$ as the left-infinite subsequence of an input up until time n, $\overleftarrow{U}$ is then the notation for all these left-infinite sequences in U. Moreover, $\overleftarrow{u}^n v := (\ldots, u_{n-2}, u_{n-1}, v)$ will symbolise the input up to time n with $v \in U$ being the specific input value at time n. The introduction of a new input at time n can be described by the mapping $\sigma_v : \overleftarrow{u}^n \mapsto \overleftarrow{u}^n v$. The right-shift map, $r\overleftarrow{U} \to \overleftarrow{U}$, of an input sequence is defined $r : (\cdots, u_{-2}, u_{-1}) \mapsto (\cdots, u_{-3}, u_{-2})$

The question now assumes the form: Can we establish a semi-conjugacy for the driven system g as presented below.

$$\begin{array}{cc} \overleftarrow{U} & \overleftarrow{U} \\ X_U & X_U. \end{array} \tag{4.2}$$

We proceed to consider a specific subclass of conjugacies.

Definition 17 (Universal Semi-Conjugacy). Given a driven system g, we call a continuous and surjective map $h : \overleftarrow{U} \to X_U$ a universal semi-conjugacy if diagram 4.2 commutes for all $v \in U$.

If the universal semi-conjugacy h exists (i.e. the diagram in 4.2 commutes) then the solution $\Psi(\bar{u})$ will intuitively have no more "complexity' than the input $\bar{u}$.

But does such a function h for the above driven system g above exist? Whenever g has the USP and $\Psi(u) = \{x_n\}_{n\in\mathbb{Z}}$ it follows that h, defined by $h(\overline{u}_n) := g(u_n, x_{n-1}) = x_n$, will satisfy the semi-conjugacy in the graph above 4.2. Regrettably, such a continuous mapping h is not guaranteed to exist when g does not have the USP [**?**, Lemma 5]. Note that even when h does exist, we are not guaranteed its injectivity. Considering again example 6, we see that even if h were to exist, it could not be injective as $X_U = \{0\}$.

Re-sketching the commutativity diagram 4.2 above by replacing X_U by its left-infinite sequence space $\overleftarrow{X}_U$, we obtain the diagram below. In this case, the function $H : \overleftarrow{U} \to \overleftarrow{X}_U$, a map that is both continuous and surjective, is called a *causal mapping* that is defined next.

Definition 18 (Causal Mapping). *A continuous, surjective map $H : \overleftarrow{U} \to \overleftarrow{X}_U$ such that*

$$H \circ \tilde{g}_v = \sigma \circ H$$

holds for all $v \in U$ where $\tilde{g}_v$ maps $(\ldots, u_{-2}, u_{-1})$ to $(\ldots, u_{-2}, u_{-1}, g(v, u_{-1}))$ is called a causal mapping.

$$\overleftarrow{U} \qquad \overleftarrow{U}$$

$$\overleftarrow{X}_U \qquad \overleftarrow{X}_U. \tag{4.3}$$

Theorem 3. *For a compactly driven system, a causal mapping H exists if and only if g has the USP.*

Proof. See [**?**, Th.3].

The driven system g can induce an embedding of $\overleftarrow{U}$ in $\overleftarrow{X}$ as follows: If the causal mapping $H : \overleftarrow{U} \to \overleftarrow{X}_U$ is injective (in addition to being surjective), it becomes the embedding of $\overleftarrow{U}$ in $\overleftarrow{X}$ induced by the driven system g. The continuity of H^{-1} follows from the fact that H is itself a continuous and surjective mapping of a compact space $\overleftarrow{U}$ in a Hausdorff space. and we refer to the map H as a *causal embedding*. [11] EdN:11

When g has the USP, the diagram below (adopted from [**?**]) illustrates the operation of the mappings h and H. The mapping $h : \overleftarrow{U} \to X_U$ is also considered an observable as mentioned in the introduction of Chapter 3).

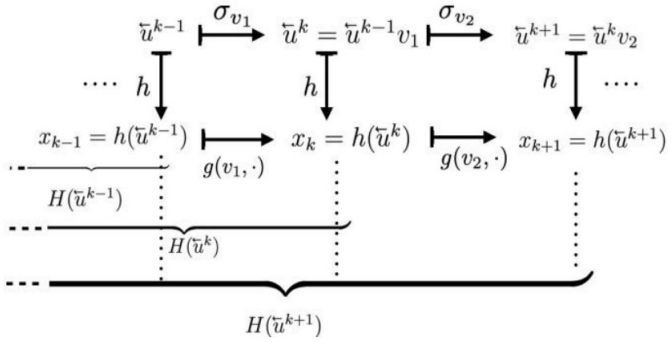

Fig. 1. Ladder-like behaviour of h and H to illustrate the causal mapping. (Figure reproduced from [**?**])

The function H contains a countably infinite number of coordinate (or factor maps) since its codomain is $\overleftarrow{X}_U$. As it is not practically feasible to consider a left-infinite sequence in X_U (in other words an element of $\overleftarrow{X}_U$) for learning, we wish to restrict the inputs we consider to a subspace of $\overleftarrow{U}$. Particularly, we restrict our attention to the so-called inverse-limit space of a dynamical system and hope to embed it within some finite product of X.

The left-infinite orbit space is significant because a great amount of information about the original system can be gleaned from its topological structure [**?**, **?**]. The formal topological structure for the inverse-limit space of a chaotic dynamical system is complicated, and further discussion is

[11] EdNote: B: edited the sentence here

relegated to [**?**, **?**]. Broadly, we may conceive of the inverse-limit system of a dynamical system as a subspace of an infinite-dimensional space where each point in the inverse-limit space corresponds to a backward orbit of the map T. Following [**?**, **?**] we provide a definition:

Definition 19 (**Inverse-Limit Space, Inverse-Limit System).** The subset $\widehat{U}_T \subset \overleftarrow{U}$ defined by

$$\widehat{U}_T := \{(\ldots, u_{-2}, u_{-1}) : Tu_i = u_{i+1}\}$$

is called the inverse-limit space of (U, T). The self-map $\widehat{T}$ induced by T on $\widehat{U}_T$ is defined by

$$\widehat{T} : (\ldots, u_{-2}, u_{-1}) \mapsto (\ldots, u_{-2}, u_{-1}, T(u_{-1}))$$

and the resulting dynamical system $(\widehat{U_T}, \widehat{T})$ is called the inverse-limit system of (U, T).

The inverse-limit space is well-defined since $T : U \to U$ is surjective by assumption. We now get to the concept of embedding the inverse limit-space of the dynamical system in $X \times X$.

Definition 20. We say a driven system g *causally embeds* a dynamical system (U, T) if it satisfies the two properties: (i) a universal semi-conjugacy exists and (ii) $H_2(\overleftarrow{u}) := (h(r\overleftarrow{u}), h(\overleftarrow{u}))$ embeds the inverse-limit space $\widehat{U}_T$ in $X \times X$.

It is imperative to take note of a subtlety here: we refer to the *map* H as a (causal) embedding,
EdN:12 whereas the driven *system* g (causally) embeds another *system* (U, T). [12]

4.4 Choosing the driven system g

So far it is not clear if the USP alone ensures the ability to causally embedding a dynamical system and we mention that a driving function g cannot just be chosen in a frivolous manner. This could possibly complicate our work.

In the above example(6), the input's temporal variation could not be related to the reachable set as X_U only consisted of a single element; little, if not no, information is encoded. To obtain a suitably complex function g, it is thus desired that the reachable set of a driven system be large enough to relate to the input. This is true even for embedding the inverse-limit space of a dynamical
EdN:13 system. [13]

To this end, we recall the notion of State-Input (SI) Invertibility.

[12] EdNote: B: inserted line
[13] EdNote: B: Expand or refer?

Definition 21 (SI-Invertibility). A driven system g is said to be SI-Invertible if $g(*, x) : U \to X$ is invertible for all $x \in X$. Alternatively it may be said that if, given x_n and x_{n-1}, u_{n-1} can be uniquely determined from $x_n = g(u_n, x_{n-1})$, then g is said to be SI-invertible.

SI-invertibility promises that 'enough' information is retained when g is chosen without introducing one's choice of g will still ensure 'enough' information is retained without introducing unwanted complexity. 'Enough' here refers to the fact that we may always recover the previous input value u_n (if we know successive states x_{n-1}, x_n).

Subsequently we define the relation Y_T induced by (U, T) on $X_U \times X_U$ for a driven system g possessing SI-invertibility. To describe the SDD formally, we consider a dynamical system $T : U \to U$ and define a relation on the reachable set X_U, i.e. a subset on $X_U \times X_U$ defined by

$$Y_T := \{(x_{n-1}, x_n) : \{x_k\}_{k\in\mathbb{Z}} \text{ is a solution for some orbit of } T \text{ and } n \in \mathbb{Z}\}.$$

The following theorem establishes the existence of a well-defined map G_T describing the single-delay dynamics(SDD) of the system above.

Theorem 4. *For an SI-invertible driven system g and a dynamical system (U, T), the map $G_T : Y_T \to Y_T$ defined by the relation $(x_{n-1}, x_n) \mapsto (x_n, x_{n+1})$ is well-defined. (This results holds even in the absence of g possessing over the USP)*

Proof. See [**?**, Th.3]

At this stage it is worth taking note of a specific driven system in the form of a discrete state-space model which has acquired some adherence in applications [**?**]- especially those pertaining to Echo State Networks and the ESP. The function

$$g(u, x) = (1 - a)x + a\overline{\tanh}(Au + \alpha Bx) \tag{4.4}$$

is SI-invertible and, if αB has a spectral norm < 1, also possesses the USP [**?**, Th.2]. It is easy to show that g is SI-invertible by recovering u_n in

$$u_{n-1} := A^{-1}\left(\overline{\tanh}^{-1}\frac{1}{a}\Big(x_{n+1} - (1 - a)x_n\Big)\right) - \alpha Bx_n \tag{4.5}$$

when x_{n-1} and x_n are known.

This specific driving function g is used in our implementation and is discussed more completely in chapter 5

Despite the ease that with which one manipulates a left-infinite history in the realm of theory, it is impossible to obtain or use such a sequence in any real-life application. Fortunately, one

does not need the entire left-infinite history of an input in practice thanks to the Uniform Attraction Property(UAP). We use an alternate version of the definition of UAP – since the notion of nonautonomous attractors in this project would take some time to establish and detracts from the principal thrust of this project, we refer to [**?**].

Definition 22 (**Uniform Attraction Property).** A driven system g has the Uniform Attraction Property (UAP) if we initialize the driven system with an arbitrary initial value $y_m \in X$, and the sequence $y_{m+1}, y_{m+2}, y_{m+3}, ...$ satisfying $y_{k+1} = g(u_k, y_k)$ for $k \geq m$ then approximates an actual solution $\{x_n\}$ uniformly in the sense that given $\epsilon > 0$ (independent of y_m) there is an integer n so that $d(x_{n+i}, y_{n+i}) < \epsilon$ for all $i \geq 0$, where $\{x_m\}$ is a solution.

The UAP guarantees that all trajectories will converge to the same trajectory as time moves forward. An illustration of this is shown in Fig. 2 where the trajectory in red locks on to the supposed actual solution when the system has the USP.

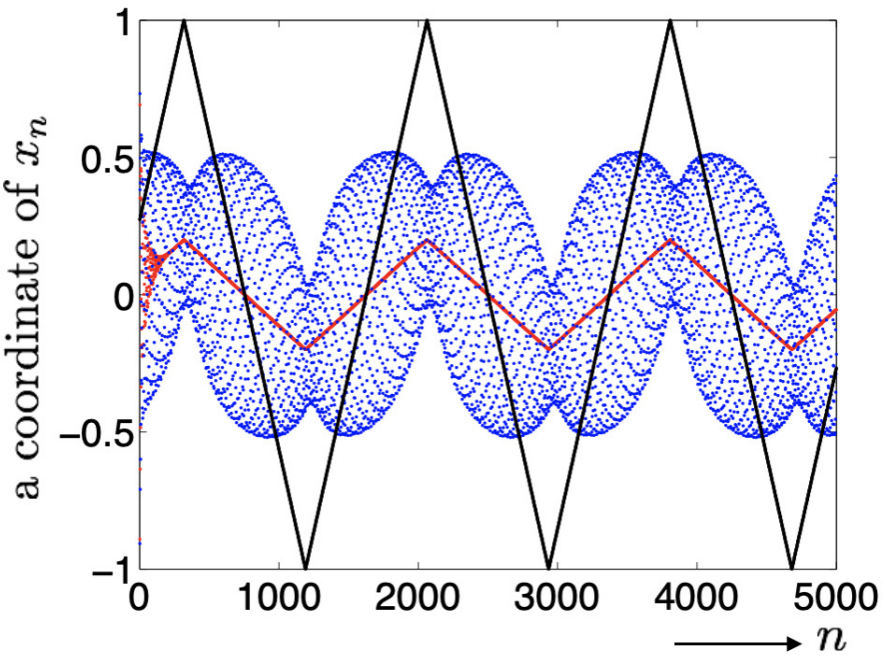

Fig. 2. A coordinate of a simulated solution $(x_0, x_1, \ldots, x_{5000})$ of a RNN plotted in red (with parameter $\alpha = 0.99$ (where g has the USP) and blue ($a = 1$ and $\alpha = 1.05$ where g does not have the USP) while the matrices A and B are randomly generated, and B has unit spectral radius. Reproduced from [**?**].

EdN:14 [14]

One may now appreciate an even more astounding result: g having the USP is equivalent to the UAP as is proved in [**?**].

[14] EdNote: B: How can I explain the black line? I don't think this makes sense to the reader immediately.

4.5 The next step in Dynamics

We are interested in determining whether $\widehat{T}$ and G_T are related. For this, we introduce the function $H_2 := (h(r\overline{u}, h(\overline{u})))$ mapping the entirety of a left-infinite sequence to some element in $X \times X$. Indeed, it may be shown that g having SI-invertibility and the USP immediately guarantees the existence of at least a semi-conjugacy between the systems (Y_T, G_T) and $(\widehat{U}_T, \widehat{T})$. This is formalised in the Causal Embedding Theorem, which we state next:

Theorem 5 (**Causal Embedding Theorem (adopted from [?])**). *Let g be a driven system with SI-invertibility and the USP. Let h denote the universal semi-conjugacy and $H_2(\overleftarrow{u}) := (h(r\overleftarrow{u}), h(\overleftarrow{u}))$, where r is the right-shift map. Let $(\widehat{U}_T, \widehat{T})$ be the inverse-limit system of a dynamical system (U, T). Then the restriction of H_2 to $\widehat{U}_T$ is a topological semi-conjugacy between the inverse-limit system $(\widehat{U}_T, \widehat{T})$ and the induced dynamical system (Y_T, G_T), i.e., the following diagram commutes*

$$\begin{array}{cc} \widehat{U}_T & \widehat{U}_T \\ \\ Y_T & Y_T. \end{array} \tag{4.6}$$

or in other words, (Y_T, G_T) is a factor of $(\widehat{U}_T, \widehat{T})$. Further, if $T : U \to U$ is a homeomorphism, then H_2 embeds $\widehat{U}_T$ in $X_U \times X_U$, and hence (Y_T, G_T) is conjugate to $(\widehat{U}_T, \widehat{T})$.

Proof. May be found as the proof of [**?**, Th.4]

Recall that H_2 maps an entire left-infinite solution sequence from Ψ to an element in $X \times X$. We are drawing nearer and nearer to our principal target and our results carry more and more weight: If we are able to learn G_T, we will also have learnt $\widehat{T}$; and since $\widehat{T}$ is an extension of T, we will have obtained T as well.

Summarising the discussing thus far:

It is easy to lose the birds-eye view, so we take a moment to review our progress up until this point.

1. We are interested in a some dynamical system (U, T) with unknown dynamics.
2. To determine properties about this system (U, T) and predict its future evolution, we determine the dynamics of the inverse-limit system $(\widehat{U}, \widehat{T})$.
3. If the driven system g is SI-invertible (and $\{u_n\} \in U$ is an orbit of T), the map G_T exists that describes the single delay dynamics.
4. If, furthermore, g has the USP, (Y_T, G_T) is semi-conjugate to $(\widehat{U}, \widehat{T})$.

5. If we can assume that T is a homeomorphism, (Y_T, G_T) is topologically conjugate to $(\widehat{U}, \widehat{T})$, an extension space of (U, T)

One can therefore in practice learn the SDD of the driven system states via G_T with enough data thanks to the USP/UAP. This enables us to do at least two things:

- Forecast $x_{n+1}, x_{n+2}, \ldots$ via iterates of G_T (if G_T can be learnt).
- Forecast future values of u_n since x_n and x_{n+1} determine u_n since g is SI-invertible.

Finally, we note that although G_T exists with SI-invertibility, we need the USP as well(see **??** below for a visual illustration). If not, the driven states would have to be running for all time since they would not have forgotten their past states.

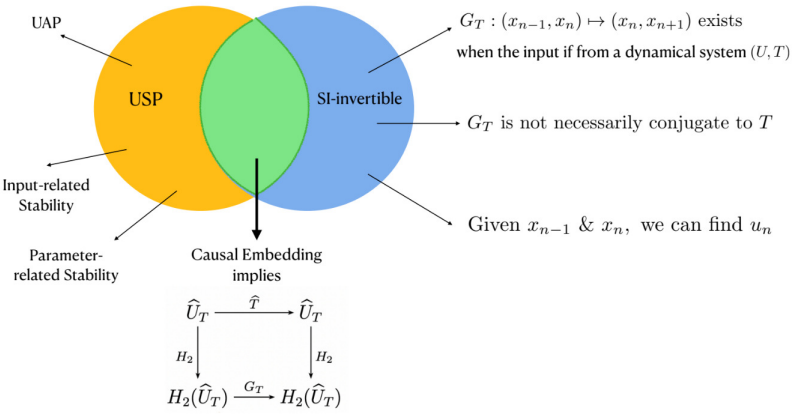

Fig. 3. Pictorial summary of results obtained up to now and how they overlap. Reproduced from **(Cite SIG-25May)**

EdN:15 [15]

4.6 A discussion of G_T

In the above sections, we established the map G_T describing the SDD of a driven system. By establishing the existence of this map, we've essentially embedded the attractor U (recall from 3.1) into the higher dimensional space $X \times X$. In layman's terms, this ensures that there is more "dimensional room" for the underlying system's underlying dynamics to "move". Since the dynamics aren't as "squashed", we might therefore hope that the dynamics of G_T are in some sense simpler than that of T. (Taken note of the fact that G_T is a homeomorphism even when T is just continuous)

[15] EdNote: Ask M: Cite SIG-25May.

In [?] it is illustrated in an empirical fashion in that the map G_T describes dynamics which are less functionally complex than that of T or of the map $\Phi_{2d,\theta}$. This is done by implementing a Recurrent Neural Network (RNN), which is discussed in 5. [16] EdN:16

We opt to learn G_T in an indirect manner by defining a new map $\Gamma : (x_{n-1}, x_n) \mapsto u_n$. It will follow immediately from G_T's existence that Γ also exists.

The reasons for taking this roundabout approach remain to be discussed in 4.7, but a pat answer may immediately be given: When Γ has been learnt, the system can be driven autonomously and then G_T is known anyway. We formalise this with a theorem.

Theorem 6. *When x_n and x_{n-1} are successive points on a solution obtained for input-orbit of T $\{u_n\}$, then the map $\Gamma : X \times X \to U$ defined by $(x_{n-1}, x_n) \mapsto u_n$ exists whenever G_T exists*

Proof. See [?, Th. 3c].

Projection mappings π_i are defined in the traditional meaning where a k-dimensional vector is projected to it's i^{th} component such that

$$\pi_i : (a_1, a_2, . , a_{k-1}, a_k) \to a_i$$

The graph in equation **??** is then extended as below:

$$\begin{array}{cc} \widehat{U}_T & \widehat{U}_T \\ \\ Y_T & Y_T \\ \\ U \times X & \end{array} \tag{4.7}$$

The problem finally simplifies to the issue of learning the map Γ and combining this with the projection mapping π_2 and the function g, which will be known. A final set of equations is obtained - equations that have been entirely constructed from data.

$$u_{k+1} = \pi_1 \circ (\Gamma, \pi_2) \circ (\pi_2, g)(u_k, x_k) \tag{4.8}$$
$$x_{k+1} = \pi_2 \circ (\Gamma, \pi_2) \circ (\pi_2, g)(u_k, x_k). \tag{4.9}$$

[16] EdNote: B: Should I add in that we'll be using Pearson coefficient?

4.7 Advantages of learning Γ

One may immediately ask why we opt to take such a roundabout route; why not just learn the map G_T from the get-go? On the surface, this seems to be an arbitrary decision path with no real reasoning, so we take a pause again and discuss the motivation for learning Gamma. There are a number of distinct advantages.

In the first place, learning Γ saves computational resources. This is due to the fact that the input u_n lies in a lower-dimensional subspace in comparison to the high-dimensional space $X \times X$.

Secondly, the function Γ is known to be stable. Learning Γ makes use of equations 4.8 which in turn employs the driven system g possessing the USP, and offers distinct advantages with regards to stability in the presence of perturbation. It is desirable that inputs that differ only slightly would have only 'slight' effects on the output of the system. Moreover, one would hope to prevent numerical errors originating from input and measurement noise (see [**?**, Th. 5]). As the data fed into the system is a function of both the input given and the parameters of the system itself (i.e. the value a, α in tanh), we exploit both input-related and parameter-related stability. Both these notions are defined by way of the continuity of an encoding map of an input and design parameter respectively in [**?**].

Informally, we may consider input-related stability as concerned with the question of whether or not small variations in input would result in small responses. If two inputs $\bar{u}$ and $\bar{u}_{noisy}$ are close in the product topology, then their tails could differ greatly due to the metric that generates the product topology has insensitivity to the differences in sequence's tails. However if the system has the USP then the function h is continuous and so $h(\bar{u}), h(\bar{u}_{noisy})$ remain close-by for small levels of noise maintaining a measure of robustness to input and measurement noise.[**?**]. In a similar fashion, parameter-related stability is obtained thanks to a result [**?**, Lemma 3.2] relating this form of stability with the ESP (which is here equivalent to the USP).

Thirdly, learning a chaotic map on a set(here Y_T) with even a small measure of noise means that the learnt system accepts arguments out of the set (Problems similar to Takens, cf. **??**). We thus have a map G_T^+ acting on Y_T^+ and since Y_T is not guaranteed to be an attractor of G_T this could lead to errors. If one learns G_T directly, we are in danger of replicating the problems arising for Takens. To see this, consider Fig. 4.

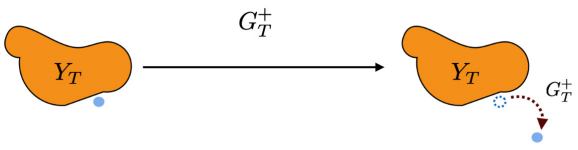

Fig. 4. Diagram of potential errors developing when G_T is learnt.

To circumvent this: if a driven system with a saturation function[17] is used, we can ensure the existence of an attractor A of the map which implements G_T, and containing Y_T^+ indirectly (via g). [18] By defining the dynamics to A, this prevents large errors from occuring. More details on the global dissipativity of g, as it is termed there, may be found in [**?**]. EdN:17 EdN:18

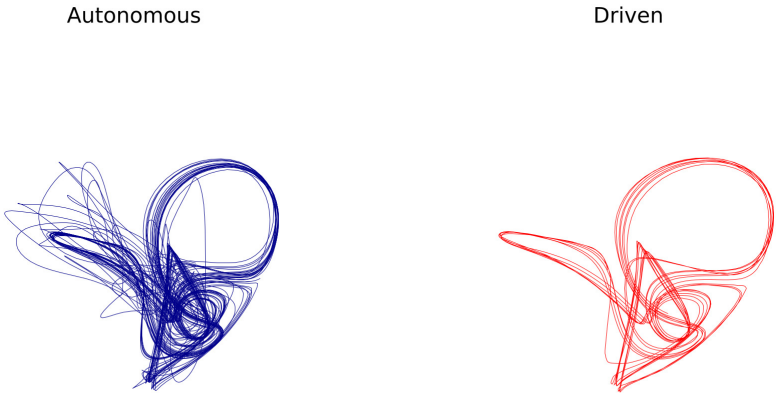

Fig. 5. Illustrating empirically the importance of global dissipativity. Plotted below are the three principal components of randomly initiated points(blue) of a learnt version of G_T versus the trajectory (x_{n-1}, x_n)(red) of driven states obtained from the Fractal Dream Attractor's data 5.3.2).

In effect, global dissipativity prevents large numerical errors due to the noise in input data from arising (see Fig. 5). If a system is not globally dissipative, neglibly small errors could lead to major inaccuracy which thus induce predictions to utterly fail.

[17] EdNote: B: What is a saturation function?

[18] EdNote: B: A little vague. Are we saying that an attractor of a map implementing G_T is also the one that contains Y_T^+?

Chapter 5

Implementation

In this chapter we turn to the implementation of the function G_T by discussing a method to learn the function Γ. We apply our methodology to some chaotic attractors. Most notably, we consider the reconstruction of the chaotic attractor of the double pendulum - an attractor that has not been successfully reconstructed because of its intricate structure. In fact the previous data-driven approaches also have not been successful in building a model from the double pendulum.

5.1 Implementing G_T

The map G_T is implemented by applying the functions Γ, g and the projection function π_2 in the relevant order as described by the equations 4.8. To reach this point, one must first learn Γ. After first normalising the data to ensure that it has zero mean value and lies within the range $[-1, 1]$ and required zero-padding(see paragraph below for further discussion), we continue by driving the system with external input through the function g.

From (4.4) we know that $g(u, x) = (1 - a)x + a\tanh(Au + \alpha Bx)$. Recall that g is SI-invertible. We refer to A as the input matrix and B the reservoir matrix.

We make use of a Recurrent Neural Network (RNN) in our implementation to project the data on
EdN:19 to a higher dimensional space, but we do not train the RNN in the conventional manner. [19] A few words about the RNNs: RNNs are widely used in the literature for temporal processing of data as a type of deep learning technique. They take the form of equations considered to be discrete-time version of continuous dynamical systems modelling a neural network of neurons [**?**].

[19] EdNote: B: Should we say what the conventional manner is?

We implement a feedforward network, (a network with no memory, unlike the RNN)[20] required to learn Γ in the *Python* programming language and making use of the *Scipy* library, alongside the *Keras* package in the *Tensorflow* library [21]. EdN:20 EdN:21

If the RNN we will be using in the next step has N neurons, then A and B are each $N \times N$ matrices. Inputs u_n of dimension $K < N$ are padded by zeroes (as remarked earlier) to embed the input in a space of dimension N. As we do not need the entire left-infinite history of input, an arbitrary initialisation of the system with initial values followed by the driving of the system with the function g means that the generated values will approach the actual solution elements in a uniform manner thanks to the UAP that we had discussed in the preceding chapter.

Thirdly we prepare the network. Utilising a network N neurons (the same value N as in the dimensions of the matrices A, B). Learning of Γ is done using the Adam Optimiser where the means square error (MSE) loss function is optimised. The system is trained several times (in our case 4) with incrementally smaller learning rates on each run (0.001 and thereafter divided by 10 at each run). Additional parameters such as the number of network-layers, neurons per layer and training-length are presented case-by-case below.

We then reach the prediction step. Making use of g's SI-invertibility and g as defined in (4.4), we have the following expression for u_n replicated from (4.5).

$$u_n := A^{-1}\left(\overline{\tanh}^{-1}\frac{1}{a}\Big(x_{n+1} - (1-a)x_n\Big)\right) - \alpha B x_n$$

The two model equations for learning from data (4.8) allows us to determine what the state x_{n+1} at time $n+1$ will be. We specifically remind ourselves of

$$x_{k+1} = \pi_2 \circ (\Gamma, \pi_2) \circ (\pi_2, g)(u_k, x_k)$$

5.2 Delay Coordinates

We also consider a more general problem of learning an attractor of dynamical system when only observations of an orbit are given. Explicitly, if (W, T) is a dynamical system with dynamics generated by $w_{n+1} = Tw_n$, and if $\theta : W \to \mathbb{R}$ is an observable, then the task is to learn a dynamical system that is topologically conjugate to (W, T) and predict $\theta(w_{m+1}), \theta(w_{m+2}), \ldots$ using

[20] EdNote: B: Expanded sentence s.t. FFN is in more context

[21] EdNote: B: Is this something you want me to write in? M: We do not implement the RNN, but the FN that learns Gamma through the Tensorflow. We called the RNN + FN set up a RCN in Adriaan's paper. FYI: FN's work only if there is a definite relationship between the u_n and u_{n+1} which is rare in temporal data. RNNs with ESP work when there is a definite relationship between $(\ldots, u_{n-1}, u_n)$ and u_{n+1} and is suited for temporal processing.

the data $\theta(w_0), \theta(w_1), \ldots, \theta(w_m)$. So how do we do it? Suppose the input generated from the delay-coordinate map $\Phi_{\theta,2d}(\theta(w_n)) := (\theta(w_{n-2d}), \ldots, \theta(w_{n-1}), \theta(w_n))$ is such that Takens delay embedding theorem (see Theorem 1) holds, in which case, there exists a homeomorphism $F_\theta : \Phi_{\theta,2d}(\theta(w_n)) \mapsto \Phi_{\theta,2d}(\theta(w_{n+1}))$. Then if we feed the input values $u_n := \Phi_{\theta,2d}(\theta(w_n))$ to a driven system g that is SI-invertible and has USP, the induced system (Y_F, G_F) would be topologically conjugate to the inverse-limit space of $(\Phi_{\theta,2d}(W), F_\theta)$ as in Theorem 5, and hence one could forecast $u_n, u_{n+1}, \ldots$. In other words, one could forecast the values $\theta(w_n), \theta(w_{n+1}), \ldots$ by feeding these observations as delay coordinates. The advantage of feeding delay-coordinates to a driven system is that the embedding is stable in the sense of global dissipativity that we have described in the previous chapter, i.e., Y_F is made to contained in an attractor of a mapping induced on Y_F that is induced by g.

We note that the twin equations together 4.8 generate a model from data. For a chaotic system, a small amount of noise due either to the input-noise or computational error would cause the solutions
EdN:22 from two accurate models with the same initial conditions to diverge as they are not identical. [22] However, statistically, they would be the same since due to ergodic theory all typical orbits have the
EdN:23 same visiting frequency to any region of the phase space of the dynamical system. [23] To illustrate that we plot the densities of the trajectories of the actual and predicted solutions.

Our implementation of the reservoir(A) and input(B) matrices in the RNN makes use of sparse matrices. We discuss three specifics relating to this concept. Firstly, the matrices are assigned a variable density in terms of the amount of non-zero entries and are scaled to have values within the range $[-1, 1]$. For this, we make use of *Python's SciPy* library and specifically the *Sparse, LinAlg* modules. In our experiments, we generally opted for a density ratio of 10%-25%. Secondly, we opted to enforce the requirement that both matrices be well-conditioned, i.e. that they have a condition number of $\tilde{1}$. The condition number of a matrix M (denoted $cond(M)$) is the product of the matrix norms of the matrix M and its inverse M^{-1} and is a measure of the sensitivity of output of a matrix
EdN:24 multiplication when an input is changed. **(Cite.)**[24] By ensuring a condition number close to 1, we also ensure that our driven function g, depending on the matrices A and B, will not be sensitive to
EdN:25 adjustments in the input. In so doing we then also guarantee another form stability. [25]

Lastly, we ensure the matrix B has unit spectral radius. This is necessary due to the Causal Embedding Theorem 5 which can then guarantee the existence of semi-conjugacy between the systems (Y_T, G_T) and $(\widehat{U}_T, \widehat{T})$. In fact, the theorem actually requires that αB have spectral radius < 1, so we impose the restriction $\alpha < 1$ and consider only the matrix B's spectral radius from thereon.

Note that to learn $\Gamma : (x_{n-1}, x_n) \mapsto u_n$ through our feedforward network, we could learn the principal components of (x_{n-1}, x_n) as well. We employ this since it provides slightly better results empirically but is not essential.

[22] EdNote: B: edited this sentence
[23] EdNote: B: I'll need to recap this sentence with you before presenting as it's new to me.
[24] EdNote: Ask M: Cite specific resource?
[25] EdNote: B: Not complete enough. Edit further and cite

Principal components are used only for a more efficient state representation to possibly reduce learning errors; it is not for a lossy approximation since we use all principal components **(Cite.)**[26]. EdN:26
More explicitly, denote $X_{1:N}$ as the matrix with the first N states of the network data represented by row vectors. If $X_{1:N} = U\Sigma P^T$[27] represents the singular value decomposition of $X_{1:N}$ [28], we then EdN:27
denote the principal component matrix P, and the principal components are given by $Z_{1:N} = X_{1:N}P$. EdN:28
These principal components are then used to train a feedforward neural network. Denote the row vectors of $Z_{1:N}$ by $z_i^T, i = 1, 2, \cdots, N$ and the neural network by NN, the network is subsequently trained to learn an approximation of the map $NN : (z_{n-1}, z_n) \mapsto u_n$. The learnt approximation of NN can be used to approximate Γ since

$$NN\left(\begin{bmatrix} P^T x_{n-1} \\ P^T x_n \end{bmatrix}\right) = NN \circ \begin{bmatrix} P^T & 0 \\ 0 & P^T \end{bmatrix} \begin{bmatrix} x_{n-1} \\ x_n \end{bmatrix} = u_n = \Gamma(x_{n-1}, x_n).$$

5.3 Experimental Results

In this section we showcase numerical results pertaining to 3 attractors that were simulated using the methodology described. We first consider a simple physical system that exhibits complicated dynamics.

5.3.1 Double Pendulum

The Double Pendulum consists of two pendulums fastened to one another such that the system moves as a whole. The first (or higher pendulum) is attached to a fixed point while the second is attached to the endpoint of the first. (See below) This system is a classical example of a system exhibiting chaos and is often used as explanation of the very well-known Butterfly Effect. [29] EdN:29
Consider again 2. The system has four variables: angle and angular velocity of each pendulum rod. An ideal system is assumed where the rods are massless and no friction in the pivots are considered.

The scalar equations of motion are derived using Newtonian physics and are reproduced from [**?**] in 5.1. Each pendulum component has an associated mass of the head, m, and length of the rod,

[26] EdNote: Ask M: Is there a specific resource to cite?
[27] EdNote: Expand here
[28] EdNote: Ask: Is there a specific resource to cite?
[29] EdNote: B: Originally though a reference here was needed, but no longer think so.

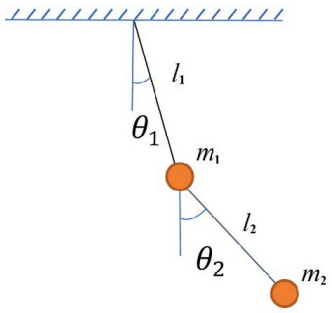

Fig. 1. Pictorial representation of the setup of a DP. Image taken from [?]

L_i. Acceleration due to gravity is denoted by g and initial velocities by $\dot{\theta}$

$$\ddot{\theta_1} = \frac{-g(2m_1 + m_2)\sin\theta_1 - m_2 g\sin(\theta_1 - 2\theta_2) - 2\sin(\theta_1 - \theta_2)m_2(\dot{\theta_2}^2 L_2 + \theta_1' L_1 \cos(\theta_1 - \theta_2))}{L_1(2m_1 + m_2 - m_2\cos(2\theta_1 - 2\theta_2))} \quad (5.1)$$

$$\ddot{\theta_2} = \frac{2\sin(\theta_1 - \theta_2)(\theta_1'^2 L_1(m_1 + m_2) + g(m_1 + m_2)\cos\theta_1 + \dot{\theta_2}^2 L_2 m_2 \cos(\theta_1 - \theta_2))}{L_2(2m_1 + m_2 - m_2\cos(2\theta_1 - 2\theta_2))} \quad (5.2)$$

The second-order system is converted to a first-order ODE system and solved using the Runge-Kutta numerical method. Here we chose the values $m_1 = 2.0$, $m_2 = 2.0$, $L_1 = 1.5$ and $m_2 = 1.5$ with initial velocities $v_1 = 1.5, v_2 = -2$ for the respective pendulum heads. Undamped DP data-sets were generated and used in this project due to the requirement that the map T be surjective that we must not forget. An example of this would be the case of a DP exhibiting energy-loss (i.e. where the map T is not surjective). In such a case, the attractor is a single point in the phase space when the double pendulum comes to rest. It must be mentioned once again that if we use data outside the attractor, learning is not reliable. To see this, consder the graphs 2 and 3.

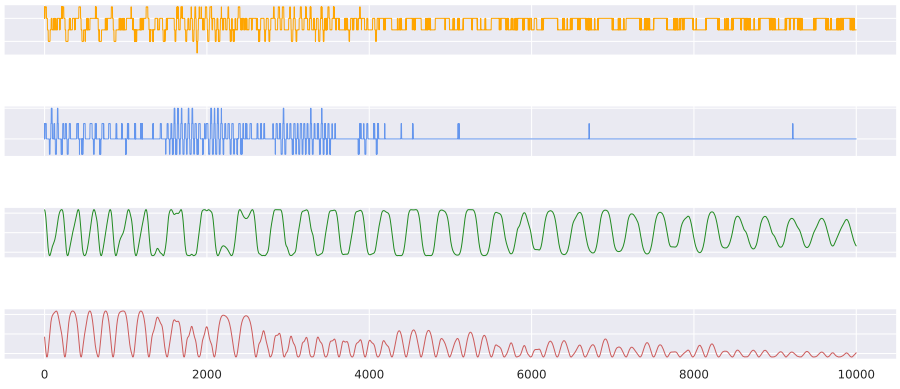

Fig. 2. x- and y-coordinates of the two pendulum heads plotted for a dataset that exhibits dying oscillations. The map generating the (four-dimensional data) for a damped pendulum is not surjective. Data obtained from chaotic double pendulum dataset generated from videos takes of experimental pendulums [?]

Having spent ample time to discuss the challenges, we now change tone so as to satisfy the optimist and present a successful run of the DP-data to predict the future movement of the pendulum.

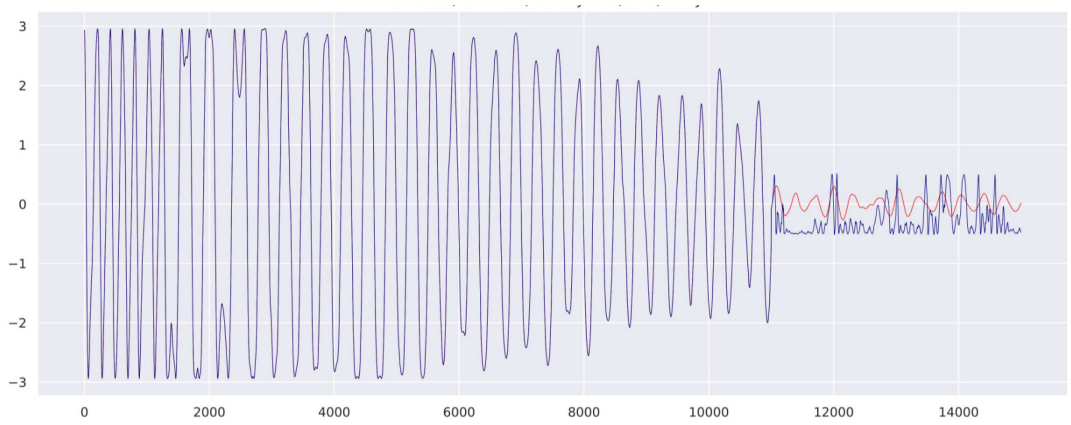

Fig. 3. Failure to forecast or learn a map which is not surjective: Evolution of the y-coordinate of the bottommost pendulum plotted here for 15000 timestep. Plotted here the predicted value(red) versus the actual value(blue). The plots overlap for the first 10000 steps, the duration of training to learn the map Γ. Afterwards, the trajectories start diverging and it the predicted value no longer accurately represents the complexity or energy-loss of the actual data.

The system was driven for 15500 steps, of which the first 500 were immediately discarded to simulate the network 'forgetting'. The driving function g had input and reservoir matrices were implemented as sparse matrices filled to 20%. Parameter-values of $\alpha = 0.99$ and $a = 0.5$ were used. The remaining 15000 datapoints were used to train a network with 128 neurons. The network was initialised to contain 16 hidden layers each with a layer dimension of 64, activated with the tanh activation function. Training was accomplished using 256 epochs with batch sizes 128 and a delay of 1. See 4 for results pertaining to the trajectory taken by the DP's components and then 5 to witness associated densities of predicted vs. actual values.

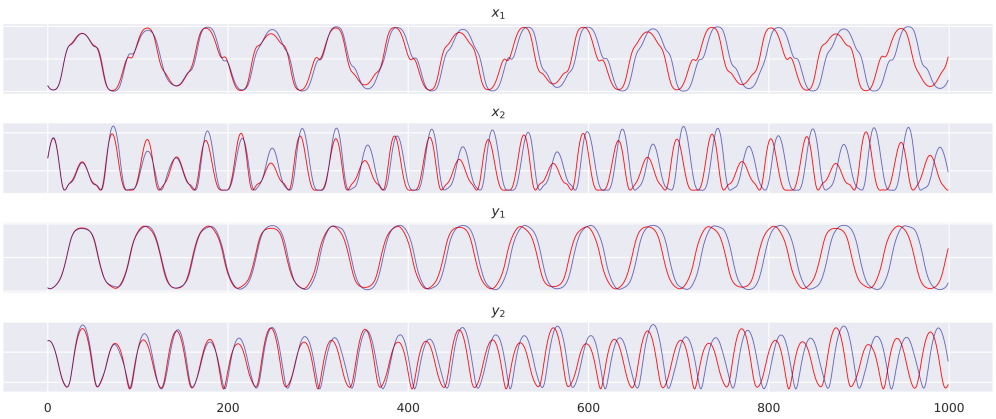

Fig. 4. Predicted(red) and actual(blue) trajectories of the x- and y-coordinates of each of the pendulum heads. From top to bottom are as follows: x-coordinate of topmost pendulum head, y-coordinate of topmost pendulum head, x-coordinate of lower pendulum head, y-coordinate of lower pendulum head. These graphs were constructed by predicting the DP 1000 timesteps into the future and in so doing illustrating the long-term consistency and accuracy of the learnt system. Here we lock onto the near-exact trajectory for about 300 timesteps and stay close up until about 600 seconds.

We now consider an experiment where noise is added to the system and find it to be incredibly robust. We employ the same parameters as before and add noise from a normal-distribution with mean zero and standard deviation equal to 0.1 which translates to roughly 39dB's of noise. (For the signal-to-noise ration we adopt the formula $\text{SNR}_{dB} = 10\log_{10}\left(\frac{P_{\text{signal}}}{P_{\text{noise}}}\right)$ where P_{signal} refers to the variance observed in the normalised data and P_{noise} represents the variance of the added noise.)

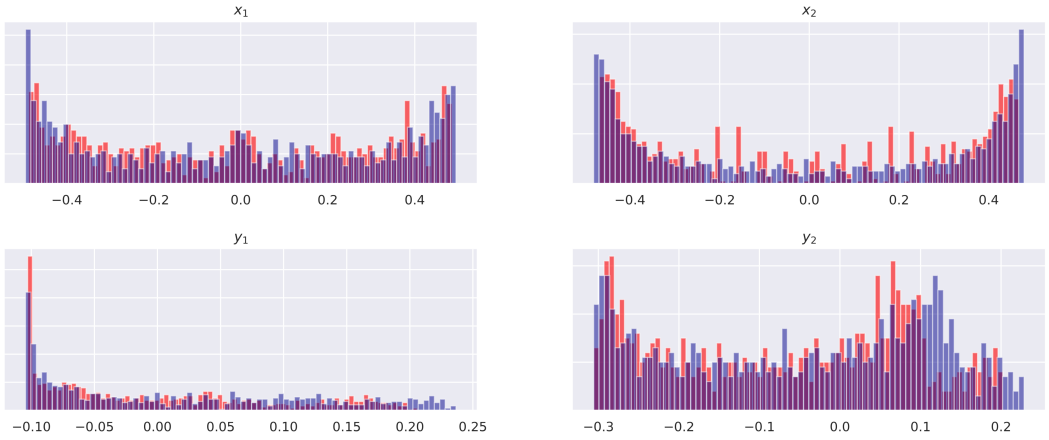

Fig. 5. Densities of predicted and actual values of x- and y-coordinate of pendulum heads.

Once again consider the actual and predicted trajectories for the noisy DP dataset in Figure 6. Next we consider the densities of the predicted and actual values in Figure 7 and observe that they display highly similar distributions.

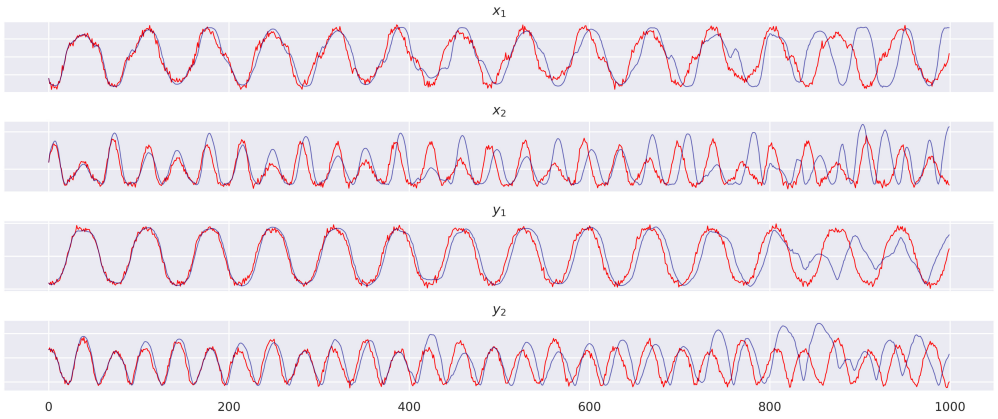

Fig. 6. Predicted(red) and actual(blue) trajectories of the x- and y-coordinates of each of the pendulum heads with noise added from a normal distribution with mean zero and standard deviation 0.1, equating to approximately 39dB's of noise. These graphs were constructed by predicting the DP 1000 timesteps into the future and in so doing illustrating the long-term consistency and accuracy of the learnt system. Here we lock onto the near-exact trajectory for about 250 timesteps and stay close up until about 400 seconds.

Lastly, a run was done where only a single coordinate (the y-coordinate of the lower pendulum head) was fed into the system and we can illustrate through the obtained success that the coordinate contains all the information in its past states necessary to forecast its future evolution. **Insert graphs here. Had to quickly change something here.**

Fig. 7. Densities of predicted and actual values of x-coordinate of first pendulum head.

5.3.2 Additional Attractors: Clifford & Thomas

We follow the methodology presented in [**?**] but opt to consider attractors different from the Lorenz system and Hénon map in this project.

Thomas' Cyclically Symmetric Strange Attractor

Thomas' Cyclically Symmetric Strange Attractor, a 3D attractor proposed in 1999 by René Thomas in [**?**], is described by a set of three equations which is distinctly reminiscent of the Lorenz system, another deterministic three-equation model exhibiting chaotic behaviour.It has a single parameter β and has been shown to transition to chaotic behavious when $\beta < 0.208186$ [**?**].

$$x_{n+1} = \sin(y_n) - \beta x_n \tag{5.3}$$
$$y_{n+1} = \sin(z_n) - \beta y_n \tag{5.4}$$
$$z_{n+1} = \sin(x_n) - \beta z_n \tag{5.5}$$

The behaviour of the system with a β-parameter value of 0.1056 was simulated by scaling it to fit inside the interval $[-1, 1]$. Two cases were considered: noise-free and the one perturbed by noise. Noise was generated from a normal distribution with mean 0 and standard deviation 0.05, which to translates approximately 33dB. (SNR_dB is calculated exactly as for the DP-data above)

A sequence of 3000 observations in both the clear and noisy data-sets respectively were fed into the system with 300 entries discarded to simulate the network's loss of memory. The next 9000 steps were predicted and compared with true data.

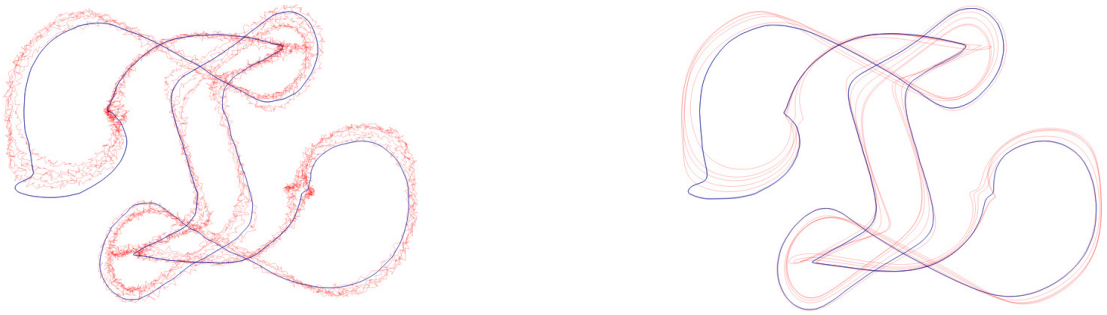

Fig. 8. True(red) and predicted(blue) trajectories for the Thomas attractor with parameter value $\beta = 0.1056$. To the left: Noise added from normal distribution with mean zero and standard deviation 0.05. Right: No noise added to dataset.

The RNN was initialised as follows: the dimension of the network is set equal to 500 neurons and 12 hidden layers of dimension 64 each were initialised. Training is realised through 150 epochs of batch sizes of 128 each; the map is learnt via the Adam Optimiser using finer and finer learning rates (0.001 and then divided by 10 at every iteration).

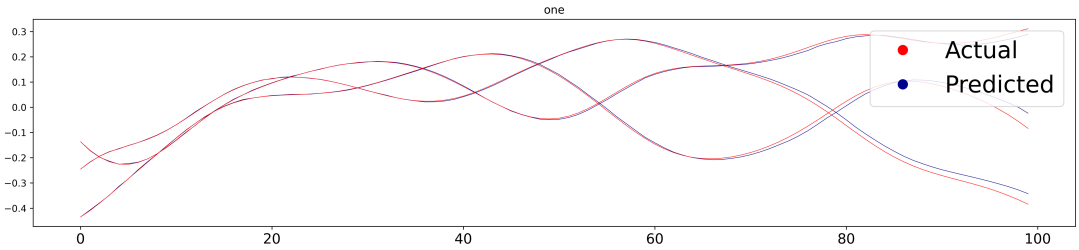

Predicted trajectories of the x- and y-coordinates for the Thomas attractor with parameter-value $\beta = 0.1056$ demonstrate empirically the ability to predict the evolution of the trajectory for the next an estimated 100 timesteps into the future near-exactly. Here no noise was added.

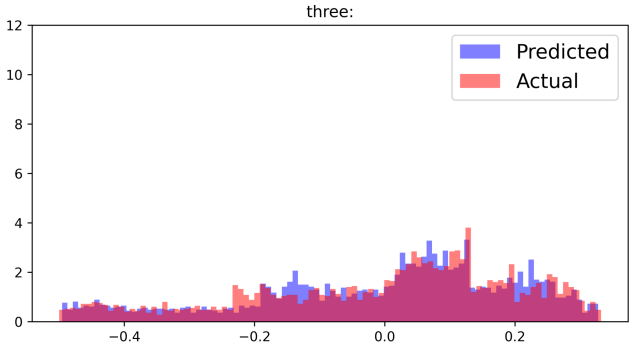

Represented here the learnt (blue) and actual (red) densities of the first coordinate (x-coordinate) of the dataset for the Cyclically Symmetric Attractor with parameter-value $\beta = 0.1056$.

Fractal Dream Attractor

Another 2-equation discrete-time map named the Fractal Dream Attractor, or more commonly known as the Pickover Map (first discovered by Clifford A. Pickover and discussed in his fascinating book "Chaos in Wonderland"[**?**]), was also considered.

$$x_{n+1} = \sin(ay_n) + c\cos(ax_n) \tag{5.6}$$
$$y_{n+1} = \sin(bx_n) + d\cos(by_n) \tag{5.7}$$

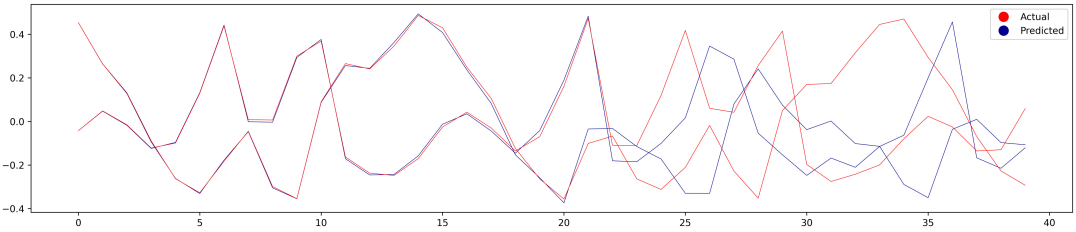

These graphs were constructed by predicting the Clifford system 1000 steps into the future and in so doing illustrating the long-term consistency and accuracy of the learnt system. As perceived here, we are able to lock on to the trajectory of the Clifford map almost exactly for the first 25 steps.

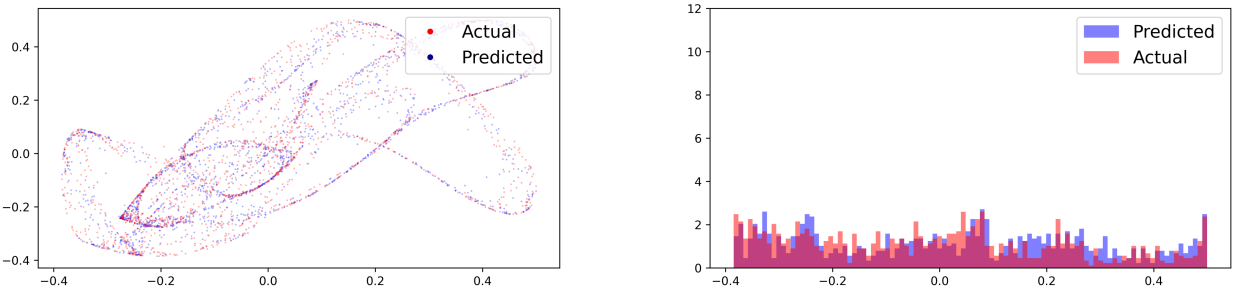

Fig. 9. The bottom row, left, shows a plot of the true attractor(red) and the predicted values(blue). Bottom row, right, shows the distribution of the first coordinate of the learnt system (blue) and the actual Clifford system (red).

The behaviour of the system with a parameter values of $x_0 = 0$, $y_0 = 0$, $a = -1.7$, $b = 1.8$, $c = -1.9$ and $d = -0.4$ was examined. Data was scaled to fit inside the interval $[-1, 1]$. Only the noise-free case was investigated. A sequence of 25000 observationswas fed into the system with 15000 entries discarded to simulate the network's loss of memory. The next 1000 steps were predicted and compared with true data. The RNN was initialised exactly as for Thomas' Cyclically Symmetric Strange attractor: the dimension of the network is set equal to 500 neurons and 12 hidden layers of dimension 64 each were initialised. Training is realised through 150 epochs of batch sizes of 128 each; the map is learnt via the Adam Optimiser using finer and finer learning rates (0.001 and then divided by 10 at every iteration).

Input	Dimension of X	u_n vs u_{n+1}	$\begin{bmatrix} x_{n-1} \\ x_n \end{bmatrix}$ vs $\begin{bmatrix} x_n \\ x_{n+1} \end{bmatrix}$
(w_n) comes from the Clifford Attractor (for $a=-1.7; b=1.8; c=-1.9; d=-0.4$): $w_{n+1} = \begin{bmatrix} \sin(aw_{n,y}) + c\cos(aw_{n,x}) \\ \sin(bw_{n,x}) + d\cos(bw_{n,y}) \end{bmatrix}$ $u_n = w_n - \overline{w}$	10	-0.21713	0.78719
	100		0.8334
	1000		0.84854

Table 5.1. Following [**?**], we determine the multidimensional correlation coefficients ρ to evidence a general reduction in the functional complexity of the map G_T emerging due to a RNN. Rows correspond to distinct dynamical systems considered in the experiments The second column corresponds to the amount of artificial neurons (the dimension of X) in the implemented RNN. The last two columns comprise numerical estimates of ρ for the relevant vectors. The linear association between u_n vs $T(u_n)$, as well as the linear relationship $\begin{bmatrix} x_{n-1} \\ x_n \end{bmatrix}$ vs $G_T\left(\begin{bmatrix} x_{n-1} \\ x_n \end{bmatrix}\right)$ may be contrasted by the reader. Finally, the RNN's dimension (from (**??**)) is provided to exhibiting that an increase in dimension of the driven system will typically result in a map G_T with less functional complexity.

.

5.4 Functional Complexity Reduction in Noninvertible maps

In the case of non-invertible maps, we note that the map G_T is a homemorphism although T is not. Further, empirically it is found that G_T is much more linear than T as measured by what is called the multidimensional correlation coefficient ρ. This coefficient is a generalization of the Pearson correlation coefficient for real-valued random variables to random vectors (see, [**?**]). We state teh details of computing this coefficient between (x_{n-1}, x_n) and $G_T(x_{n-1}, x_n)$. If Σ_a and Σ_b denotes the covariance matrices of the vectors (x_{n-1}, x_n) and $G_T(x_{n-1}, x_n)$ respectively, and if Σ_{ab} denotes the covariance matrix between the vectors (x_{n-1}, x_n) and $G_T(x_{n-1}, x_n)$, then the multidimensional correlation coefficient is computed by using the traces of these matrices:

$$\rho = \frac{\mathrm{tr}(\Sigma_{ab})}{\mathrm{tr}(\sqrt{\Sigma_a \Sigma_b})}.$$

This multidimensional correlation coefficient satisfies one of the desired and well-known properties of the one-dimensional Pearson coefficient. That is, $\rho = \pm 1$ if and only if $Y \overset{d}{=} AX + b$ for some invertible matrix A and vector b. Hence ρ, and in practice can be used to measure the linear relationship between two random vectors of the same dimension and thus serves as an indicator of functional complexity. For the non-invertible system defined by the Clifford attractor, we indicate the difference by which ρ changes for G_T in Table 5.4. Following [**?**], we say that this multidimensional correlation coefficients ρ to evidence a general reduction in the functional complexity of the map G_T emerging due to a RNN. In the Table 5.4, the second column corresponds to the amount of artificial neurons (the dimension of X) in the implemented RNN.

Chapter 6

Conclusion

Chapter 7

Conclusions

There are a myriad of techniques to generate accurate models for observed dynamical systems using data obtained from measurement functions. Core to the success of such methods is the fact that we can often characterise the dynamics from am observed space by a mapping of much lower functional complexity when compared to the true map describing the unknown underlying system. Takens theorem and the numerous generalizations thereof is one such method establishing (under some generic conditions) the learnability of a system produced by creating a delay-coordinate vector from a sufficiently large number of previous observations from a dynamical system. In this case the new system is topologically conjugate to the system from which the observed time-series was obtained. A critical concern of such methods is the requirement of full knowledge of the underlying state space variables governing the dynamical system one is interested in. In real-world conditions this information is rarely available and, when it is, is often contingent upon human expertise and insight.

Each discrete-time state space model has at its core a driven dynamical system. In this project, it has been shown that an input originating from a compact space entailing exactly one solution (i.e., if the driven system has the USP) is equivalent to representing information without distortion, a concept which was formalised by establishing the existence of a causal mapping's. The established results are general, implying that any driven dynamical system with specific properties, such SI-invertibility, can give rise to a causal mapping. In particular, we have a topological conjugacy (semi-conjugacy) between the data comprising the single-delay lag dynamics of a driven system [**?**] and the underlying homeomorphic dynamical system. Finite-length input data is shown to be sufficient for forecasting as the left-infinite segment of the past of the input beyond some arbitrarily large but finite time (a result which holds due to the universal semi-conjugacy of a driven system's continuity) influences the driven system's states in an almost negligibly small manner.

Viewed through the lens of reservoir computing, we have also demonstrated that when single-delay dynamics are utilised, a learnable map in a reservoir computing network certainly exists. Moreover, within a reservoir computing network, such a driven system posssesses certain proven qualities pertaining to the robustness of the system to different forms of perturbation. We are thus able to preserve the quality of a representation that would otherwise have remained sensitive to various fluctuations and rendering the learning of the system's dynamics wholly unpredictable.

Finally, we have considered some physical systems to observe the methodology in practice and verify that we can indeed predict the future evolution of chaotic systems such as the double pendulum. We demonstrated the robustness of our methodology to external noise by considering the cases of the Dream Attractor and the Double Pendulum.

[30] EdN:30

[30] EdNote: Loose paragraph commented out